Final comment should be devoted to the calculated vibrational frequencies. At the HF/6-31G* level, the shift in the frequency of the N-N stretching in **3** is $\Delta\nu = -51$ cm^{-1} compared to the N_2 molecule. The reported experimental value is $\Delta\nu = -133$ cm^{-1}.[3] We believe that inclusion of the electron correlation is necessary to obtain a reasonable agreement for $\Delta\nu$. For the CO adduct, the calculations yield $\Delta\nu = -42$ cm^{-1}.

Conclusions

The results of HF/6-31G* and MP2/6-31G* calculations demonstrate high reactivity of the borabenzene molecule toward carbon monoxide and nitrogen. The adduct formed between borabenzene and carbon monoxide exhibits a remarkable stability. The nitrogen adduct, though less stable, should be isolable. The reactivity of borabenzene can be attributed to a donation from the nonbonding σ^0 orbital of either CO or N_2 to the low-lying vacant σ^* orbital of borabenzene. Relief of the strain within the borabenzene ring can further contribute to the exothermicity of the addition reactions. The charge distribution in both free borabenzene and its adducts seems to be better rationalized within the GAPT population analysis than the Bader one.

Acknowledgment. This research has been performed under the auspices of the US DOE.

Ab Initio SCF MO and Natural Bond Orbital Studies of 7-Silanorbornadiene and 7,7-Dimethyl-7-silanorbornadiene. Two Molecules Possessing an Inverted Sequence of π Orbitals

Michael N. Paddon-Row,*,† Stephen S. Wong,† and Kenneth D. Jordan*,‡

Contribution from the School of Chemistry, University of New South Wales, P.O. Box 1, Kensington, New South Wales 2033, Australia, and Department of Chemistry, University of Pittsburgh, Pittsburgh, Pennsylvania 15260. *Received January 17, 1989*

Abstract: The geometries of norbornadiene, **1**, 7-silanorbornadiene, **2**, and 7,7-dimethyl-7-silanorbornadiene, **3**, have been optimized at the HF/STO-3G and HF/3-21G levels (within C_{2v} symmetry constraint). In addition, **2** has also been optimized by using the 3-21G(*) basis set which contains a set of polarization functions on Si. It was found that, although the π canonical MOs (CMOs) of **1** followed the natural sequence, i.e., π_+ (a_1) below π_- (b_1), the inverted sequence is observed (i.e., π_+ above π_-) for both **2** and **3**. Through-bond (TB) orbital interactions are therefore more important than through-space (TS) orbital interactions in **2** and **3**. The π^* CMOs, on the other hand, followed the natural sequence in all three molecules. Orbital interactions in **1** and **2** were dissected into TS and TB components by using the Weinhold natural bond orbital (NBO) localization procedure. It is found that TS interactions are weaker in **2** than in **1**, owing to the former molecule having a larger dihedral angle (120°) for the six-membered ring compared to **1** (114°). In addition, TB coupling to the π_+ orbital (which raises that level) is substantially larger in **2** than in **1**, an effect that is attributed to the more electropositive nature of silicon compared to carbon. The combination of weakened TS interactions and strengthened TB interactions is sufficient to cause the inverted sequence of π levels in **2** (and in **3**). TB and TS effects are found to reinforce each other in the π^* manifolds of both **1** and **2**; consequently, an inverted sequence of π^* levels is unlikely to be found in any type of simple norbornadiene molecule. The NBO analysis of interactions in the π manifold showed that σ/π interactions dominate over σ^*/π interactions. However, both σ^*/π^* and σ/π^* interactions should be considered in the analysis of TB coupling in the π^* manifold, with the former being slightly larger than the latter.

Recent experimental studies[1] have demonstrated the occurrence of unusually rapid intramolecular electron transfer between donor and acceptor groups fixed at predetermined distances, by rigid polynorbornyl spacers. Such rapid rates were attributed to a strong through-bond coupling mechanism between the donor and acceptor orbitals with those of the polynorbornyl framework.[1e] In order to obtain a more detailed understanding of the coupling factor which is responsible for these large rates, we have undertaken both experimental and theoretical investigations of a series of model dienes with the two double bonds separated by norbornylogous spacer groups. Particular emphasis has been placed on the splittings between the π cation and between the π^* anion states of these compounds. These splittings, which provide a measure of the electronic coupling between the donor and acceptor groups (both ethylenic in the model compounds), figure prominently in the theory of electron transfer. In the present work, we examine in detail the simplest member of this series of model compounds, norbornadiene, **1**, and consider as well 7-silanorbornadiene, **2**, and 7,7-dimethyl-7-silanorbornadiene, **3**. Specifically, we explore the utility of localized orbital methods for analyzing the contributions of through-bond (TB) and through-space (TS) interactions to the splittings between the π cation and between the π^* anion states.[2]

Norbornadiene **1** has become a paradigm for a molecule that exhibits dominant through-space (TS) orbital interactions within both π and π^* manifolds.[2-8] This is a consequence of the structurally enforced propinquity of the double bonds in **1** (they

† University of New South Wales.
‡ University of Pittsburgh.

(1) (a) Closs, G. L.; Calcaterra, L. T.; Green, N. J.; Penfield, K. W.; Miller, J. R. *J. Phys. Chem.* **1986**, *90*, 3673. (b) Penfield, K. W.; Miller, J. R.; Paddon-Row, M. N.; Cotsaris, E.; Oliver, A. M.; Hush, N. S. *J. Am. Chem. Soc.* **1987**, *109*, 5061. (c) Hush, N. S.; Paddon-Row, M. N.; Cotsaris, E.; Oevering, H.; Verhoeven, J. W.; Heppener, M. *Chem. Phys. Lett.* **1985**, *117*, 8. (d) Warman, J. M.; de Haas, M. P.; Paddon-Row, M. N.; Cotsaris, E.; Hush, N. S.; Oevering, H.; Verhoeven, J. W. *Nature (London)* **1986**, *320*, 615. (e) Oevering, H.; Paddon-Row, M. N.; Heppener, M.; Oliver, A. M.; Cotsaris, E.; Verhoeven, J. W.; Hush, N. S. *J. Am. Chem. Soc.* **1987**, *109*, 3258. (f) Joran, A. D.; Leland, B. A.; Geller, G. G.; Hopfield, J. J.; Dervan, P. B. *J. Am. Chem. Soc.* **1984**, *106*, 6090. (g) Joran, A. D.; Leland, B. A.; Felker, P. M.; Zewail, A. H.; Hopfield, J. J.; Dervan, P. B. *Nature (London)* **1987**, *327*, 50.

(2) (a) Hoffmann, R. *Acc. Chem. Res.* **1971**, *4*, 1. (b) Hoffmann, R.; Heilbronner, E.; Gleiter, R. *J. Am. Chem. Soc.* **1970**, *92*, 706.

(3) Dewar, M. J. S.; Wasson, J. S. *J. Am. Chem. Soc.* **1970**, *92*, 3506.

(4) Heilbronner, E.; Schmelzer, A. *Helv. Chim. Acta* **1975**, *58*, 936.

(5) Bischof, P.; Hashmall, J. A.; Heilbronner, E.; Hornung, V. *Helv. Chim. Acta* **1969**, *52*, 1745.

(6) Heilbronner, E.; Martin, H.-D. *Helv. Chim. Acta* **1972**, *55*, 1490.

(7) Heilbronner, E. *Israel J. Chem.* **1972**, *10*, 143.

(8) Jordan, K. D.; Michejda, J. A.; Burrow, P. D. *Chem. Phys. Lett.* **1976**, *42*, 227.

0002-7863/90/1512-1710$02.50/0

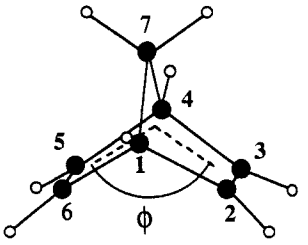

1

○ hydrogen ● carbon

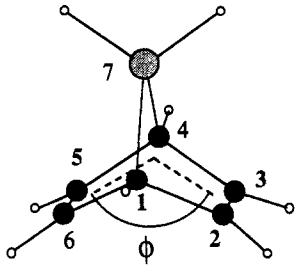

2

○ hydrogen ● carbon ○ silicon

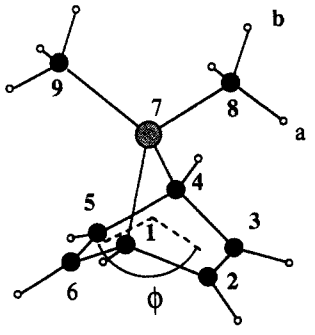

3

○ hydrogen ● carbon ◉ silicon

are only ca. 2.4 Å apart[9]) which ensures strong interorbital overlap between the basis π (π_a and π_b) and π^* (π_a^* and π_b^*) orbitals associated with the double bonds. Direct TS interactions place the energy of the positive combination of π orbitals, π_+ ($= 1/\sqrt{2}(\pi_a + \pi_b)$) of a_1 symmetry, below that of the negative combination, π_- ($= 1/\sqrt{2}(\pi_a - \pi_b)$) of b_1 symmetry (norbornadiene has C_{2v} symmetry). Likewise, the energy of $\pi_+^*(b_2)$ lies below that of $\pi_-^*(a_2)$. Such a level sequence, i.e., $E(\pi_-) > E(\pi_+)$ and $E(\pi_-^*) > E(\pi_+^*)$, where, for example, $E(\pi_-)$ represents the energy of the π_- orbital, has been called the natural sequence of orbitals[6] and always obtains for dominant TS interactions. This orbital sequence for **1** has been verified both theoretically[2-4,10,11] and experimentally, principally by electron transmission (ET) spectroscopy[8] and photoelectron (PE) spectroscopy[5,6] for the π^* and π levels, respectively. The ET spectrum of **1** showed a large π^* splitting energy of 1.52 eV,[8] which was attributed to TS interactions, and a series of elegant PE studies on a variety of norbornadienes revealed not only a large π_+/π_- splitting energy of 0.86 eV for **1** but also confirmed that the π $^2B_1$ cation state does indeed lie below the π $^2A_1$ cation state.[6,7]

It has been known for quite some time that through-bond (TB) orbital interactions[2a,12-15] between the π orbitals and the σ bonds of the norbornadienyl framework must also play an important role in determining the magnitude of the π level splitting in **1**.[3,4,7] Thus a MINDO/2 study on **1** carried out by Dewar and Wasson[3] revealed that the π splitting calculated for **1** was considerably enlarged if TB interactions were deliberately suppressed in the calculation (by deleting, from the Fock matrix, interactions between the π orbitals and the σ orbitals centered on C1, C4, and C7). This result suggests that TB and TS interactions in **1** oppose each other, with the former tending to generate an inverted sequence of π levels,[4] i.e., $E(\pi_+) > E(\pi_-)$. The origin of the opposing nature of TB and TS effects in **1** has been delineated by Heilbronner and Schmelzer through application of their heuristically useful model for quantitatively analyzing TB and TS interactions.[4] This analysis, which will be described in more detail below, clearly demonstrates that TS interactions between the π orbitals in **1** are substantially larger than the overall π splitting energy, thereby demonstrating the opposing tendencies of TS and TB interactions. Moreover, their analysis shows that, whilst smaller than TS interactions, TB interactions in **1** are nevertheless, significant. This naturally leads one to enquire how norbornadiene can be modified, perhaps by a combination of structural and electronic factors (but without resorting to the addition of either extra unsaturated groups or groups bearing nonbonding orbitals), such that an inverted sequence of π (or π^*) levels would result. In this paper we present one possible solution to this enquiry. We describe results of an ab initio MO study on 7-silanorbornadiene, **2**, and 7,7-dimethyl-7-silanorbornadiene, **3**, which reveal an inverted sequence of π levels in both molecules but a natural sequence of π^* levels.

Computational Details

In decomposing interactions into TB and TS contributions, it is important to recognize that such decomposition is not unique. However, by adopting a well-prescribed procedure, such as that of Heilbronner and Schemelzer, we believe that it is possible to gain important insight into the factors contributing to the relative energies of the π (and π^*) levels of complex molecules. Furthermore, this approach should also permit one to make meaningful comparisons of the relative magnitudes of TB and TS interactions along series of related compounds just as the Mulliken population analysis has proven very useful for analyzing trends in atomic charges.

All calculations were carried out by using the GAUSSIAN 82 and GAUSSIAN 86 suites of programs.[16] Full geometry optimizations of **1**–**3** (C_{2v} symmetry constraint) were carried out at the restricted Hartree–Fock (HF) level by using the Schlegel analytical gradient procedure[17] and the split-valence 3-21G basis set.[18a] Optimized structures for **2** and **3** using the minimal STO-3G basis set[18b] were also determined as these were used as starting points for the 3-21G optimizations. Optimized geometrical parameters for **1**–**3** are given in Table I, together with total energies. Whilst this work was in progress, Rauk and co-workers reported the HF/3-21G optimized structure for **1**,[19a] which is identical with that reported here. Moreover, Rauk and co-workers carried out harmonic frequency calculations for the optimized structure of **1** and verified that

(9) (a) Dallinga, G.; Toneman, L. H. *Recl. Trav. Chim. Pays-Bas* **1968**, *87*, 805. (b) Yokozeki, A.; Kuchitsu, A. *Bull. Chem. Soc. Jpn.* **1971**, *44*, 2356.
(10) Balaji, V.; Jordan, K. D.; Burrow, P. D.; Paddon-Row, M. N.; Patney, H. K. *J. Am. Chem. Soc.* **1982**, *104*, 6849.
(11) Balaji, V.; Ng, L.; Jordan, K. D.; Paddon-Row, M. N.; Patney, H. K. *J. Am. Chem. Soc.* **1987**, *109*, 6957.
(12) Hoffmann, R.; Imamura, A.; Hehre, W. J. *J. Am. Chem. Soc.* **1968**, *90*, 1499.
(13) Gleiter, R. *Angew. Chem., Int. Ed. Engl.* **1974**, *13*, 696.
(14) Paddon-Row, M. N. *Acc. Chem. Res.* **1982**, *15*, 245.
(15) Paddon-Row, M. N.; Jordan, K. D. *Molecular Structure and Energetics*; Liebman, J. F., Greenberg, A., Eds.; VCH Publishers: New York, NY, 1988; Vol 6, Chapter 3.
(16) (a) Binkley, J. S.; Frisch, M. J.; DeFrees, D. J.; Raghavachari, K.; Whiteside, R. A.; Schlegel, H. B.; Fluder, E. M.; Seeger, R.; Pople, J. A. GAUSSIAN 82; Carnegie-Mellon University: Pittsburgh, PA 15213. (b) Frisch, M. J.; Binkley, J. S.; Schlegel, H. B.; Raghavachari, K.; Melius, C. F.; Martin, R. L.; Stewart, J. J. P.; Bobrowicz, F. W.; Rohlfing, C. M.; Kahn, L. R.; DeFrees, D. J.; Seeger, R.; Whiteside, R. A.; Fox, D. J.; Fleuder, E. M.; Pople, J. A. GAUSSIAN 86; Carnegie-Mellon Quantum Chemistry Publishing Unit: Pittsburgh, PA, 1984.
(17) Schlegel, H. B. *J. Comput. Chem.* **1982**, *3*, 214.
(18) (a) Binkley, J. S.; Pople, J. A.; Hehre, W. J. *J. Am. Chem. Soc.* **1980**, *102*, 939. (b) Hehre, W. J.; Stewart, R. F.; Pople, J. A. *J. Chem. Phys.* **1969**, *51*, 2657. (c) Møller, C.; Plesset, M. S. *Phys. Rev.* **1934**, *46*, 618. Pople, J. A.; Binkley, J. S.; Seeger, R. *Int. J. Quantum Chem., Symp.* **1976**, *10*, 1. Krishnan, R.; Pople, J. A. *Int. J. Quantum Chem.* **1978**, *14*, 91. Krishnan, R.; Frisch, M. J.; Pople, J. A. *J. Chem. Phys.* **1980**, *72*, 4244.
(19) (a) Castro, C. R.; Butler, R.; Rauk, A.; Wieser, H. *J. Mol. Struct. (Theochem)* **1987**, *152*, 241. (b) For 4-31G geometry optimization of **1** see: Wiberg, K. B.; Bonneville, G.; Dempsey, R. *Israel J. Chem.* **1983**, *23*, 85.

Table I. HF/3-21G and HF/STO-3G Optimized Geometrical Parameters[a] and Energies[b] (E) for the C_{2v} Structures **1**, **2**, and **3**, Together with the π_+, π_-, π_+^*, and π_-^* Canonical MO Energies[c] and Their Splitting Energies,[c] Δ and Δ^*

	1	2			3	
parameter	3-21G	3-21G	3-21G(*)	STO-3G	3-21G	STO-3G
C1–X7	1.566	1.949	1.911	1.882	1.961	1.888
C1–C2	1.550	1.539	1.542	1.542	1.536	1.541
C2–C3	1.319	1.325	1.325	1.315	1.325	1.315
C2–C6	2.480	2.474	2.479	2.463	2.467	2.459
C8–Si					1.911	1.861
C1–H	1.076	1.076	1.076	1.083	1.077	1.083
C2–H	1.069	1.070	1.070	1.081	1.070	1.081
X7–H	1.081	1.490	1.477	1.424		
C8–H_a					1.083	1.081
C8–H_b					1.087	1.083
C2–C1–C6	106.2	107.0	107.0	106.0	106.9	105.9
C1–X7–C4	92.0	79.1	80.8	80.7	78.4	80.3
C1–C2–C3	107.5	112.1	112.0	111.3	112.1	111.3
H–C1–X7	118.2	123.2	123.9	123.1	123.3	123.2
H–C2–C3	128.1	125.9	125.8	126.4	125.8	126.4
H–X7–H	111.7	109.3	109.1	109.7		
C8–Si–C9					108.3	109.1
H_a–C_8–Si					111.4	111.6
H_b–C8–Si					110.5	111.0
H–C2–C3–C4	177.9	179.0	179.4	178.4	179.2	178.6
H_b–C8–Si–H_a					120.6	120.3
ϕ	114.0	120.4	120.2	118.0	120.3	117.9
$-E^b$	268.16187	517.91532	518.01052	514.63280	595.60065	591.82663
$E(\pi_-)(b_1)^c$	−8.72 (−7.44)[e]	−9.04	−9.09	−7.42	−8.83	−7.35
$E(\pi_+)(a_1)^c$	−9.76 (−8.26)[e]	−8.88	−8.94	−7.25	−8.62	−7.13
$\Delta^{c,d}$	1.04 (0.82)[e]	−0.16	−0.15	−0.17	−0.21	−0.22
$E(\pi^*)(a_2)^c$	6.28 (9.81)[e]	5.84	5.68	9.93	5.93	9.98
$E(\pi_+^*)(b_2)^c$	4.29 (8.04)[e]	3.39[f]	3.72	8.23	4.23	8.32
$\Delta^{*\,c,d}$	1.99 (1.77)[e]	2.45	1.96	1.70	1.69	1.66

[a] Bond lengths in Å; bond angles and dihedral angles are in deg. [b] Energies in au (1 au = 627.51 kcal/mol). [c] Orbital energies and splitting energies in eV (1 eV = 23.06 kcal/mol). [d] $\Delta = E(\pi_-) - E(\pi_+)$; $\Delta^* = E(\pi_-^*) - E(\pi_+^*)$. A negative sign for Δ means that the π_+ level lies above the π_- level. [e] The quantities in parentheses are the STO-3G values (at the 3-21G optimized geometries). [f] There is another 3-21G orbital of b_2 symmetry having an energy of 5.80 eV. Both b_2 orbitals contain nearly equal admixture of π and bridge C–Si–C orbitals.

it does correspond to an energy minimum. Although harmonic frequency calculations on **2** and **3** were not carried out, the overall structural similarity of **1**, **2**, and **3** strongly suggests that the C_{2v} structures for the latter two molecules should also correspond to energy minima.

Although the analysis in this paper is based on the molecular orbital picture, the relevant experimental quantities are the ionization potentials and electron affinities. Hence, we assume the validity of Koopmans' theorem (KT) and associate the energies of the cation and anion states with the negatives of the filled and unfilled, canonical molecular orbitals, respectively. With the STO-3G and 3-21G basis sets the energies of the anion states thus estimated are much too high. However, we note that for our present purpose the quantities of primary interest are the relative and not the absolute energies of the π and π^* levels. We have found in previous studies on norbornadiene and other nonconjugated dienes that the splittings between the π^* anion states and between the π cation states calculated at a KT/STO-3G level of theory are in good agreement with the experimental splittings.[11] Because the anion states of norbornadiene, **1**, and 7-silanorbornadiene, **2**, lie energetically above the ground states of the neutral molecules, the virtual orbitals have positive energies and will not converge to unique values as the basis sets are enlarged. Indeed, the virtual orbitals will "collapse" onto continuum solutions if flexible basis sets are employed. The use of a small basis set (e.g., STO-3G) prevents this problem.

Structures

The HF/3-21G structure of **1** has already been discussed by Rauk and co-workers.[19a] Suffice it to say that agreement between the computed and the experimentally determined structures is quite good.[9,19] Although the synthesis of several 7-silanorbornadienes has been reported,[20-27] their structures have not been determined experimentally (or theoretically for that matter). Although a check on the reliability of our HF/3-21G optimized structures for **2** and **3** cannot therefore be made, we are confident that the structures for **2** and **3** are sufficiently reliable for the purpose in hand, the worst error probably being an overestimation of the C–Si bond lengths by ca. 0.05 Å.[28] Because the 3-21G(*) basis set, which contains d functions on Si,[28] is known to give equilibrium C–Si bond lengths in good agreement with experimental values,[28,29] the structure of **2** was reoptimized at this level (Table I). As expected, inclusion of polarization functions on Si resulted in contraction in the lengths of the Si–C bonds (by 0.04 Å) and Si–H bonds (by 0.01 Å). However, because the remaining optimized geometrical parameters and, more importantly, the π and π^* orbital energy splittings are found to be mainly unaffected by the inclusion of the Si d functions, the ensuring discussion of the structures of **1–3** will be based on the 3-21G results, unless stated otherwise.

The 3-21G geometries of **2** and **3** display several interesting features. The C1–Si bond in these molecules is about 0.04 Å longer than that calculated (1.917 Å) for CH_3SiH_3[28] and $CH_3SiH_2CH_3$.[30] This result is probably not an artifact of the calculation since the C8–Si bond length in **3** is quite normal (at the STO-3G level, the C1–Si bond is still longer than the C8–Si bond but by only 0.03 Å). The C1–C7 bond length (1.566 Å) in **1** is likewise longer than usual (cf., 1.541 Å in propane[31]). The

(20) Laporterie, A.; Dubac, J.; Mazerolles, P.; Lesbre, M. *Tetrahedron Lett.* **1971**, 4653.
(21) Barton, T. J.; Witiak, J. L.; McIntosh, C. L. *J. Am. Chem. Soc.* **1972**, *94*, 6229.
(22) Maruca, R.; Fischer, R.; Roseman, L.; Gehring, A. *J. Organomet. Chem.* **1973**, *49*, 139.
(23) Balasubramanian, R.; George, M. V. *J. Organomet. Chem.* **1975**, *85*, 131.
(24) Mayer, B.; Neumann, W. P. *Tetrahedron Lett.* **1980**, *21*, 4887.
(25) Barton, T. J.; Goure, W. F.; Witiak, J. L.; Wulff, W. D. *J. Organomet. Chem.* **1982**, *225*, 87.
(26) Appler, H.; Gross, L. W.; Mayer, B.; Neumann, W. P. *J. Organomet. Chem.* **1985**, *292*, 9.
(27) Marinetti-Migrani, A.; West, R. *Organometallics* **1987**, *6*, 141.
(28) Pietro, W. J.; Francl, M. M.; Hehre, W. J.; DeFrees, D. J.; Pople, J. A.; Binkley, J. S. *J. Am. Chem. Soc.* **1982**, *104*, 5039.
(29) Boatz, J. A.; Gordon, M. S.; Hilderbrandt, R. L. *J. Am. Chem. Soc.* **1988**, *110*, 352.
(30) Paddon-Row, M. N. Unpublished results.
(31) *Carnegie-Mellon Quantum Chemistry Archive*, 3rd ed; Whiteside, R. A., Frisch, M. J., Pople, J. A., Eds.; Carnegie-Mellon University: Pittsburgh, PA, 1983.

anomalous C1–C7 bond length in **1** is also apparent from the electron diffraction structure for **1**.[9b] Presumably a combination of strain and hyperconjugative electron donation from the C1–X7 and C4–X7 σ MOs to the π^* MOs is responsible for the long C1–X7 and C4–X7 bond lengths in **1–3**.

The small value of 92° for the C1–C7–C4 angle in **1** is symptomatic of the strain present in this ring system. The C1–Si–C4 angle in **2** and **3** is even smaller (ca. 79°) than that found for **1**. Related to this is the finding that the dihedral angle, ϕ, associated with the six-membered ring, is about 6° larger in **2** and **3** than in **1** (this difference is 4° using the STO-3G basis set). These trends can be explained in terms of simple geometrical and strain arguments. If the geometry of **2** were identical with that calculated for **1**, with the exception of retaining the equilibrium C–Si bond lengths, then the C1–Si–C4 angle would be only 70°, some 10° smaller than that found for optimized **2**. This is a highly strained angle (the HF/3-21G equilibrium C–Si–C angle for $CH_3SiH_2CH_3$ is 112°)[30] and can be relieved by increasing the value of ϕ, since this leads to a concomitant increase in the C1–C4 distance. Apparently, the optimized value of 120° for ϕ represents a compromise between diminishing C1–Si–C4 angle strain and diminishing C1–Si and C4–Si bond strengths, resulting from reduced overlap between the orbitals on Si and those on C1 and C4, with increasing ϕ. In summary, our calculations on **2** and **3** are indicative of the presence of substantial strain associated with the C1–Si–C4 group. These results are entirely consistent with the known thermal lability of the C1–Si and C4–Si bonds in many 7-silanorbornadienes.[20-27]

Orbital Interactions

Energies of the canonical (i.e., fully delocalized) π and π^* MOs, CMOs, (i.e., ${}^{CM}\pi_-$, ${}^{CM}\pi_+$, ${}^{CM}\pi_-^*$, and ${}^{CM}\pi_+^*$) for **1–3** are given in Table I, together with the corresponding splitting energies, $\Delta = E(\pi_-) - E(\pi_+)$, and $\Delta^* = E(\pi_-^*) - E(\pi_+^*)$. A positive value for the splitting energy means that a natural sequence of orbitals obtains. The data for **1** show that TS interactions are dominant in both π and π^* manifolds. The 3-21G π splitting energy for **1**, in the Koopmans' theorem approximation,[32] is 1.04 eV which gives a π-ionization splitting energy 0.18 eV larger than the experimental value (0.86 eV[5]). Better agreement is obtained with the minimal STO-3G basis set which gives a Δ value of 0.82 eV. A similar situation obtains for the Δ^* splitting energy, with the STO-3G value (1.77 eV) being in better agreement with the experimental value (1.52 eV[8]) than the 3-21G value (1.99 eV).

In marked contrast to **1**, Δ is *negative* for both **2** and **3**; −0.16 eV for **2** and −0.21 eV for **3** at the HF/3-21G level of theory. Similar values of Δ are obtained at the HF/STO-3G and HF/3-21G(*) levels of theory. The insensitivity of Δ for **2** to the basis set strongly suggests that the result is not a calculational artifact. We have also carried out unrestricted third-order Møller–Plesset (UMP3) calculations[18c] on the two cation states of **2** by using both the 3-21G(*) and 6-31G* basis sets and the HF/3-21G(*) geometry of the neutral molecule. These calculations place the ${}^2A_1$ cation state about 0.27 eV below the ${}^2B_1$ cation state. Hence, even though the state splitting is quite small, we feel confident about the predicted state ordering. We conclude that TB interactions dominate over TS interactions in the π manifolds of both **2** and **3** and that the splitting of their π-ionization bands should be smaller than that for **1** but with the vertical ${}^2B_1$ cation radical state lying *above* the ${}^2A_1$ cation radical state at the geometry of the neutral. Interestingly, the Δ^* splitting energies for **2** and **3** are positive, thereby showing that, for the π^* orbitals, TS interactions are more important than TB interactions.

The origin of the reversal of the relative importance of TS and TB interactions on the π levels in **2** and **3**, compared to **1**, is attributed to a combination of two factors, the first being geometrical and the other electronic. The geometrical factor concerns the magnitude of ϕ since TS interactions are strongly attenuated with increasing values of this parameter, as a result of diminishing π,π orbital overlap.[3,4,7] Because TB effects are less sensitive to ϕ (the loss in overlap of the π MOs with the σ orbitals of the six-membered ring, with increasing ϕ, is compensated by a gain in overlap with the C1–X7–C4 bridge σ orbitals), there should be a critical value for ϕ for which TB effects become dominant. By using the MINDO/2 semiempirical method, this critical value of ϕ was calculated to be ca. 116° for **1**[3] and ca. 140° for 1,4-cyclohexadiene.[7,33]

The geometrical factor was explored by carrying out a series of single-point 3-21G calculations on **1** and **2** for values of ϕ ranging from 112° to 124° (all other geometrical parameters were kept fixed at their equilibrium values). The π and π^* CMO energies together with the associated splitting energies are given in Table II. The π_- and π_+ levels for **1** follow the natural sequence for all values of ϕ studied, and extrapolation of the data indicates that the crossover point corresponds to $\phi \approx 130°$. This result is in marked contrast to that of the MINDO/2 study[3] which predicts a much smaller crossover value of ϕ ($\approx$116°). However, because most INDO/CNDO based semiempirical methods overestimate TB effects at the expense of TS interactions.[3,4] we believe that our ab initio data present a more reliable picture of the dependence of Δ on ϕ. This conviction is reinforced by the observation that the Δ value for **1** calculated in the MINDO/2 approximation by using the experimental geometry is almost an order of magnitude smaller than the experimental value (0.86 eV[5]).[3] Clearly, the MINDO/2 method is not correctly giving the relative magnitudes of TB and TS interactions in **1**. For **2**, the HF/3-21G calculated crossover value occurs at $\phi = 118.5°$ and is much smaller than that estimated for **1**. Thus, the computed inverted sequence of π levels found for **2** and **3** is due, in part, to the somewhat larger equilibrium value of ϕ for these molecules, compared to **1**, for if ϕ for **2** and **3** happened to be similar to that found for **1** (i.e., 114°), a significant TS dominated Δ value of ca. 0.46 eV would then result. The fact that the crossover value of ϕ for **1** is much larger than that for **2** suggests that TB interactions in **1** are substantially weaker than in the latter molecule.

The electronic factor mainly influences TB interactions and may be visualized by using the following simple argument. From a perturbational MO point of view, one may introduce TB interactions into the scheme through mixing π_+ (a_1 symmetry) and π_- (b_1 symmetry) with appropriately constructed symmetry-adapted semilocalized σ MOs (σ SLMOs), as described by Heilbronner and Schmelzer.[4] If we ignore contributions from C and Si core atomic orbitals and focus attention only on the valence shell orbitals, then **1** and **2** are each associated with 36 SLMOs, which are schematically drawn in Figure 1. The SLMOs are generated through mixing of localized two-center orbitals of the same type, that is, these localized orbitals are related to each other by the symmetry operations of the point group to which the molecule belongs. Of these SLMOs, 12 are of a_1 symmetry, eight are of b_1 symmetry, 10 are of b_2 symmetry, and six are of a_2 symmetry. Also included in Figure 1 are the π_+, π_-, π_+^*, and π_-^* SLMOs, which will henceforth be designated by ${}^{SL}\pi_+$, ${}^{SL}\pi_-$, ${}^{SL}\pi_+^*$, and ${}^{SL}\pi_-^*$, respectively, in order to distinguish them from the final fully delocalized CMOs (${}^{CM}\pi_+$, ${}^{CM}\pi_-$, ${}^{CM}\pi_+^*$, and ${}^{CM}\pi_-^*$).

Consider, first, TB interactions involving ${}^{SL}\pi_+$ and ${}^{SL}\pi_-$ shown, respectively, by α_7 and β_5 in Figure 1. Because the energy gap separating the π and the virtual σ^* orbitals in **1** and **2** is considerably larger than that separating the π and σ orbitals (by ca. 13 eV at the HF/3-21G level), it is reasonable to assume that σ/π mixing will be energetically much more significant than σ^*/π mixing, and, therefore, we can ignore the latter (this will be further justified below). There are six occupied σ SLMOs of a_1 symmetry $\{\alpha_i, i = 1, ..., 6\}$ that can mix with ${}^{SL}\pi_+$ ($\equiv \alpha_7$) and four of b_1 symmetry $\{\beta_i, i = 1, ..., 4\}$ that can mix with ${}^{SL}\pi_-$ ($\equiv \beta_5$). By using a crude argument based purely on the number of σ SLMOs that are available for mixing, it would appear then that the energy level of ${}^{SL}\pi_+$ should be affected much more strongly than the ${}^{SL}\pi_-$ level. More quantitatively, it has been shown[4] that the σ SLMOs constructed from the C–C bonds, namely, α_2, α_4, and β_3 make the major contributions to TB coupling in **1**. Both ${}^{SL}\pi_+$ and ${}^{SL}\pi_-$

(32) Koopmans, T. *Physica* **1933**, *1*, 104.

(33) Bischof, P. Dissertationarbeit, Universität Basel, 1971.

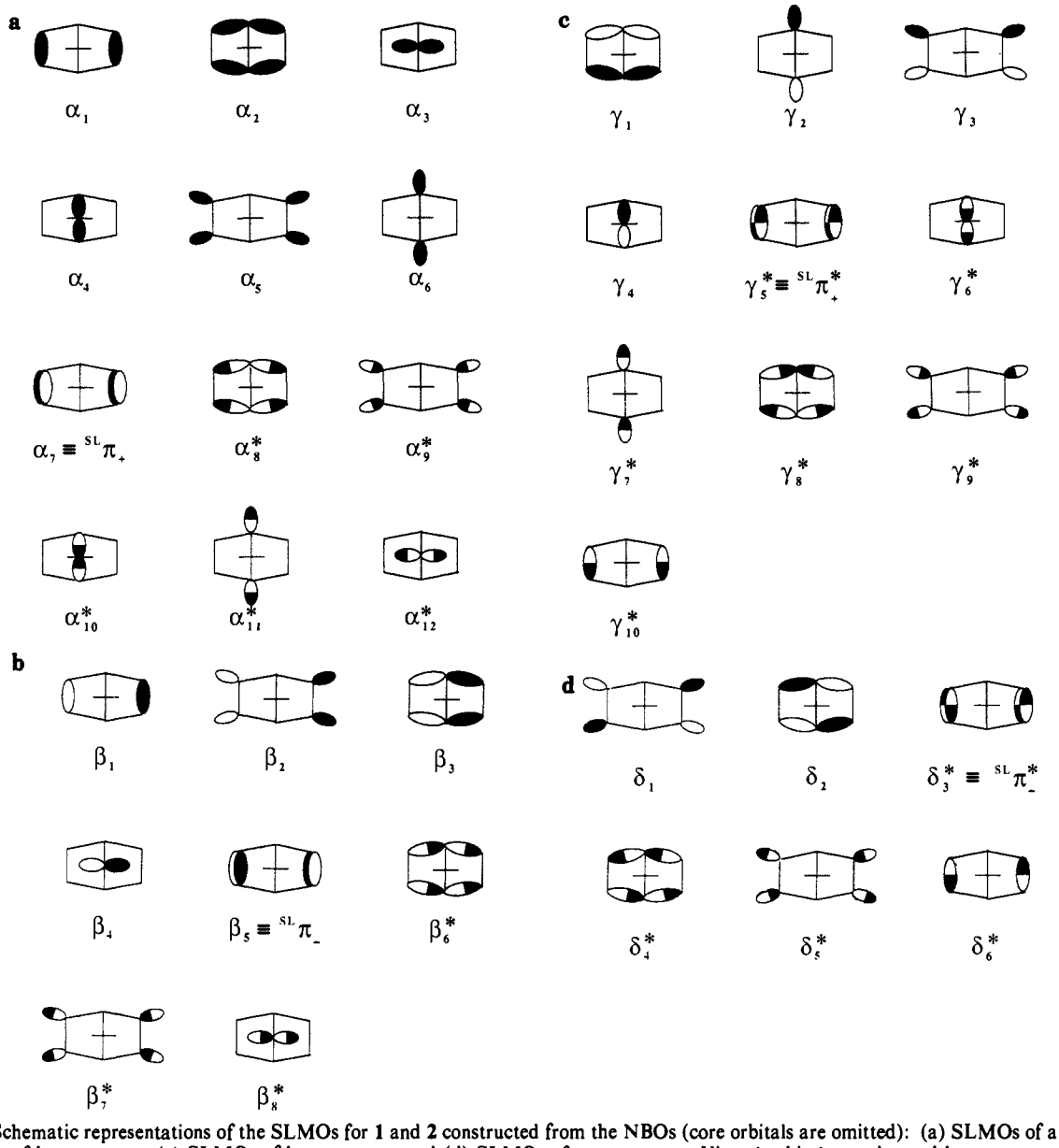

Figure 1. Schematic representations of the SLMOs for **1** and **2** constructed from the NBOs (core orbitals are omitted): (a) SLMOs of a_1 symmetry; (b) SLMOs of b_1 symmetry; (c) SLMOs of b_2 symmetry; and (d) SLMOs of a_2 symmetry. Virtual orbitals are denoted by a superscript asterisk.

levels are raised through this mixing, although the former should be more affected than the latter because there is no counterpart to α_4 in the $\{\beta_i\}$ set of SLMOs. Thus, TB interactions in **1**, by themselves, lead to an inverted sequence of π levels. Replacement of C7 in **1** by Si should have little effect on the energies and shapes of orbitals α_2 and β_3 because X7 makes no contribution to these orbitals. Consequently, TB interactions should raise the ${}^{SL}\pi_-$ level in **1** and **2** by comparable amounts (it will be shown below that the different value of ϕ for **1** and **2** has little influence on the magnitude of TB interactions). On the other hand, replacement of C7 by the more electropositive Si atom will raise the self-energy of orbital α_4 and will polarize this orbital more toward C1 and C4. This polarization will lead to a greater orbital overlap between ${}^{SL}\pi_+$ and the σ SLMO α_4 in **2** compared to **1**. It follows from second-order perturbation theory that both effects combine to increase the amount of TB coupling for π_+ in **2** compared to **1**. Net TB interactions, i.e., the difference between the ${}^{SL}\pi_-$ and ${}^{SL}\pi_+$ levels resulting *exclusively* from TB effects, should, therefore, be larger for **2** (and **3**) than for **1**.

Turning to interactions between π^* orbitals, it is seen from Table II that the Δ^* values for both **1** and **2** are considerably larger than the corresponding Δ values and that the natural sequence of π^* levels obtains for all values of ϕ considered, even for **2**. This rather surprising lack of tendency of the π^* levels to follow an inverted sequence is probably due to the fact that the π^* SLMOs (${}^{SL}\pi_+^*$ and ${}^{SL}\pi_-^*$), unlike the corresponding π SLMOs, couple fairly strongly with *both* σ and σ^* SLMOs.[11] From Figure 1c, it is seen that destabilization of the ${}^{SL}\pi_+^*$ ($\equiv \gamma_5^*$) level through mixing with the lower lying four σ SLMOs ($\gamma_1 - \gamma_4$) partially offsets mixing with the higher lying five σ^* SLMOs ($\gamma_6^* - \gamma_{10}^*$). Likewise, the destabilizing influence of the two a_2 σ SLMOs, δ_1 and δ_2, on the ${}^{SL}\pi_-^*$ ($\equiv \delta_3^*$) level is tempered by the stabilization caused through mixing with the three σ^* SLMOs ($\delta_4^* - \delta_6^*$). The ${}^{SL}\pi_+^*$ and ${}^{SL}\pi_-^*$ levels are therefore not as much influenced by TB effects as are the corresponding ${}^{SL}\pi_+$ and ${}^{SL}\pi_-$ levels, with the result that TS effects predominate for the range of values of ϕ studied herein. The situation regarding 1,4-cyclohexadiene, for which $\phi = 180°$, is not yet resolved.[34]

The above reasoning can be placed on a quantitative basis by dissecting the net orbital interactions into TS and TB components along the lines originally suggested by Heilbronner and Schmelzer.[4] A wide variety of molecules has been studied by using this analysis[4,35] or a slightly modified version thereof.[36] The

(34) HF/STO-3G calculations[43] indicate a normal sequence of π^* orbitals for 1,4-cyclohexadiene (D_{2h} symmetry). Also the original ET spectroscopic study of this molecule was interpreted in terms of a normal sequence of π^* orbitals.[8] However, HF/3-21G calculations predict an inverted sequence of π^* levels, and recent electron energy loss spectroscopic studies (P. D. Burrow, personal communication) also appear to be consistent with an inverted ordering.

Table II. HF/3-21G Energies[a] of the π_-, π_+, π_-^*, and π_+^* Canonical MOs and the Corresponding Splitting Energies, Δ and Δ^*,[a] for **1** and **2** as a Function of the Flap Angle ϕ (deg)

		ϕ						
		112°	114°	116°	118°	120°	122°	124°
		π Manifold[a]						
1	$E(\pi_-)$	-8.63	-8.72	-8.81	-8.89	-8.96	-9.02	-9.08
	$E(\pi_+)$	-9.84	-9.76	-9.70	-9.63	-9.56	-9.50	-9.44
	Δ[b]	1.21	1.04	0.89	0.74	0.60	0.48	0.36
2	$E(\pi_-)$	-8.57	-8.69	-8.81	-8.92	-9.04	-9.12	-9.21
	$E(\pi_+)$	-9.24	-9.15	-9.06	-8.98	-8.88	-8.82	-8.73
	Δ[b]	0.67	0.46	0.25	0.06	-0.16	-0.30	-0.47
		π^* Manifold[a]						
1	$E(\pi_-^*)$	6.39	6.28	6.17	6.07	5.97	5.88	5.79
	$E(\pi_+^*)$	4.25	4.29	4.33	4.36	4.39	4.43	4.46
	Δ^*[b]	2.14	1.99	1.85	1.71	1.58	1.45	1.33
2	$E(\pi_-^*)$	6.34	6.21	6.09	5.97	5.84	5.75	5.65
	$E(\pi_+^*)$	3.28	3.31	3.34	3.36	3.39	3.41	3.43
	Δ^*[b]	3.06	2.90	2.75	2.61	2.45	2.34	2.22

[a] Energies in eV. [b] $\Delta = E(\pi_-) - E(\pi_+)$; $\Delta^* = E(\pi_-^*) - E(\pi_+^*)$. A negative value for $\Delta(\Delta^*)$ implies that the $\pi_+(\pi_+^*)$ level lies above the $\pi_-(\pi_-^*)$ level.

essential methodology of the Heilbronner–Schmelzer approach which, to date, has been used only for analyzing interactions between occupied orbitals is as follows. The N occupied canonical (fully delocalized) SCF MOs (CMOs) of a closed shell 2N electron molecule are transformed into a set of orthogonal localized (largely two-center) orbitals (LMOs) according to a prescribed localization procedure.[37] If the molecule contains two interacting π MOs, then we denote the π CMOs by ${}^{CM}\pi_+$ and ${}^{CM}\pi_-$ and the corresponding LMOs by ${}^{L}\pi_a$ and ${}^{L}\pi_b$. The π LMOs, now localized on different double bonds, a and b, are essentially isolated from one another and also from the σ LMOs. Therefore, ${}^{L}\pi_a$ and ${}^{L}\pi_b$ form a suitable basis upon which TS and TB interactions may be built to form the final π CMOs, π_+ and π_-. In this context, the following elements of the Fock matrix in the basis of the LMOs are important:

$$E({}^{L}\pi_a) = {}^{L}F_{aa} = \langle {}^{L}\pi_a|F|{}^{L}\pi_a\rangle \quad (1)$$

$$E({}^{L}\pi_b) = {}^{L}F_{bb} = \langle {}^{L}\pi_b|F|{}^{L}\pi_b\rangle \quad (2)$$

$${}^{L}F_{ab} = \langle {}^{L}\pi_a|F|{}^{L}\pi_b\rangle \quad (3)$$

where $E({}^{L}\pi_a)$ and $E({}^{L}\pi_b)$ are the self-energies of ${}^{L}\pi_a$ and ${}^{L}\pi_b$, respectively, and ${}^{L}F_{ab}$ is a measure of the interaction energy between ${}^{L}\pi_a$ and ${}^{L}\pi_b$. This interaction energy must, perforce, be exclusively of the TS kind if ${}^{L}\pi_a$ and ${}^{L}\pi_b$ are *truly* localized (see below, however). The set of N occupied LMOs is then transformed into a set of symmetry-adapted semilocalized σ and π MOs (SLMOs), by mixing together "equivalent" LMOs that are related to each other by the symmetry operations of the molecular point group. Thus, for norbornadiene, the SLMOs are α_1–α_7, β_1–β_5, γ_1–γ_4 and δ_1–δ_2 (Figure 1). This operation transforms ${}^{L}\pi_a$ and ${}^{L}\pi_b$ into

$${}^{SL}\pi_+ = 1/\sqrt{2}({}^{L}\pi_a + {}^{L}\pi_b) \quad \text{and} \quad {}^{SL}\pi_- = 1/\sqrt{2}({}^{L}\pi_a - {}^{L}\pi_b)$$

This transformation formally represents the incorporation of TS interactions between the π orbitals into the scheme. If ${}^{L}\pi_a$ and ${}^{L}\pi_b$ are degenerate (which is the case for **1**–**3**), then the self-energies of ${}^{SL}\pi_+$ and ${}^{SL}\pi_-$ are given by

$$E({}^{SL}\pi_+) = E({}^{L}\pi_a) + {}^{L}F_{ab} \text{ and } E({}^{SL}\pi_-) = E({}^{L}\pi_a) - {}^{L}F_{ab} \quad (4)$$

and the TS interaction energy between the π orbitals, Δ_{TS}, is

$$\Delta_{TS} = -2{}^{L}F_{ab} \quad (5)$$

Note that we are adopting the convention of positive orbital overlap between the π LMOs. Consequently, the matrix element of the interaction, ${}^{L}F_{ab}$, is negative, and Δ_{TS} is positive.

The total contribution made by TB interactions, Γ, to each π CMO level is given by the energy difference between a particular π CMO (which contains both TS and TB effects) and the respective SLMO of the same symmetry (which contains only TS interactions). Thus

$$\Gamma_+ = E(\pi_+) - E({}^{SL}\pi_+) \quad \text{and} \quad \Gamma_- = E(\pi_-) - E({}^{SL}\pi_-)$$

Note that a positive (negative) value for Γ means that TB interactions cause the appropriate π SLMO to be raised (lowered). By performing yet another transformation, this time to the set of σ SLMOs, a set of orthogonal precanonical σ MOs (PCMOs) is generated,[4] from which the total TB interactions can be resolved into various contributions from the different σ relay PCMOs. These contributions are obtained from the appropriate Fock matrix elements for the interactions between the ${}^{SL}\pi$ SLMOs and the σ PCMOs, by using second-order perturbation theory. Alternatively, TB interactions can be analyzed through appropriate deletion of elements from the Fock matrix in the basis of the LMOs,[36] a method which we will employ herein (vide infra).

To date, the quantitative analysis of orbital interactions has been carried out by using either the Edmiston–Ruedenberg[37a] or the Foster–Boys[37b] orbital localization procedures. Moreover, in these investigations,[4,35,36,51] only the filled, and not the virtual orbitals, were localized, which meant that only those interactions between filled orbitals, and not those between virtual orbitals, could be analyzed. Such a localization procedure is too restrictive for our present requirements as we are interested in interactions between the π^* orbitals as well as those between the π orbitals. Also, useful insights into the energetic significance of interactions between filled and virtual orbitals, such as σ/π^* and σ^*/π interactions, cannot be obtained by localizing the filled orbitals alone.[38] Clearly, the *complete* set of CMOs, that is both filled and virtual sets, should be localized in order to circumvent these restrictions. Although the Foster–Boys method can be used to generate both filled and virtual LMOs,[37c] the method, at least as implemented in the GAUSSIAN 86 suite of programs,[16b,39] is not suited to the present study. This is because the two sets of filled and virtual CMOs are localized separately, to give the respective sets of filled and virtual LMOs. It then follows that all matrix elements between filled and virtual LMOs are necessarily zero. Consequently, these LMOs cannot be used to investigate interactions between filled and virtual orbitals; in a sense, each of these LMOs already incorporates such interactions, for reasons similar to those given in footnote 38 below. In view of this problem, we therefore chose to use the method of natural bond orbitals (NBOs) for the localization procedure. The NBO procedure, developed by the Weinhold group,[40] represents an ab initio wave function

(35) Honegger, E.; Heilbronner, E.; Wiberg, K. B. *J. Electron Spectrosc. Relat. Phenom.* **1983**, *31*, 369.

(36) (a) Imamura, A.; Ohsaku, M. *Tetrahedron* **1981**, *37*, 2191. (b) Imamura, A.; Tachibana, A.; Ohsaku, M. *Ibid.* **1981**, *37*, 2793. (c) Imamura, A.; Hirao, K. *Ibid.* **1979**, *35*, 2243. (d) Ohsaku, M.; Imamura, A.; Hirao, K.; Kawamura, T. *Ibid.* **1979**, *35*, 701. (e) Ohsaku, M.; Imamura, A.; Hirao, K. *Bull. Chem. Soc. Jpn.* **1978**, *51*, 3443.

(37) (a) Edmiston, C.; Ruedenberg, K. *Rev. Mod. Phys.* **1963**, *35*, 457. (b) Foster, J. M.; Boys, S. F. *Rev. Mod. Phys.* **1960**, *32*, 300. (c) Cizek, J.; Förner, W.; Ladik, J. *Theor. Chim. Acta* **1983**, *64*, 107.

(38) This problem is somewhat more complicated than given above because the filled LMOs already contain some admixture from idealized localized virtual (i.e., σ^*) orbitals, as the following simple argument illustrates. Consider a set of truly localized (nonorthogonal) two-center localized orbitals (TLOs) {core, σ, π, lone pairs, σ^*, π^*} that one intuitively uses when applying the Hoffmann conceptual model. If one assumes that this set spans the Hilbert space of the AO basis set used, then it is possible to express the occupied CMOs in terms of the set of TLOs. Consequently, any set of filled orthogonal LMOs generated by the Edmiston–Ruedenberg or the Foster–Boys procedures likewise can be expressed in terms of these TLOs. Since the latter comprises of virtual as well as filled orbitals, it follows that the filled LMOs must contain some admixture of virtual TLOs. The point, of course, is that LMOs are not TLOs but are slightly delocalized over other atomic centers. These "tails" arise both from the demands of LMO orthogonality and also from the admixture of virtual TLOs. This point has been nicely illustrated by Reed and Weinhold by using their method of natural localized molecular orbitals.[40c]

(39) Frisch, M. J. Personal communication.

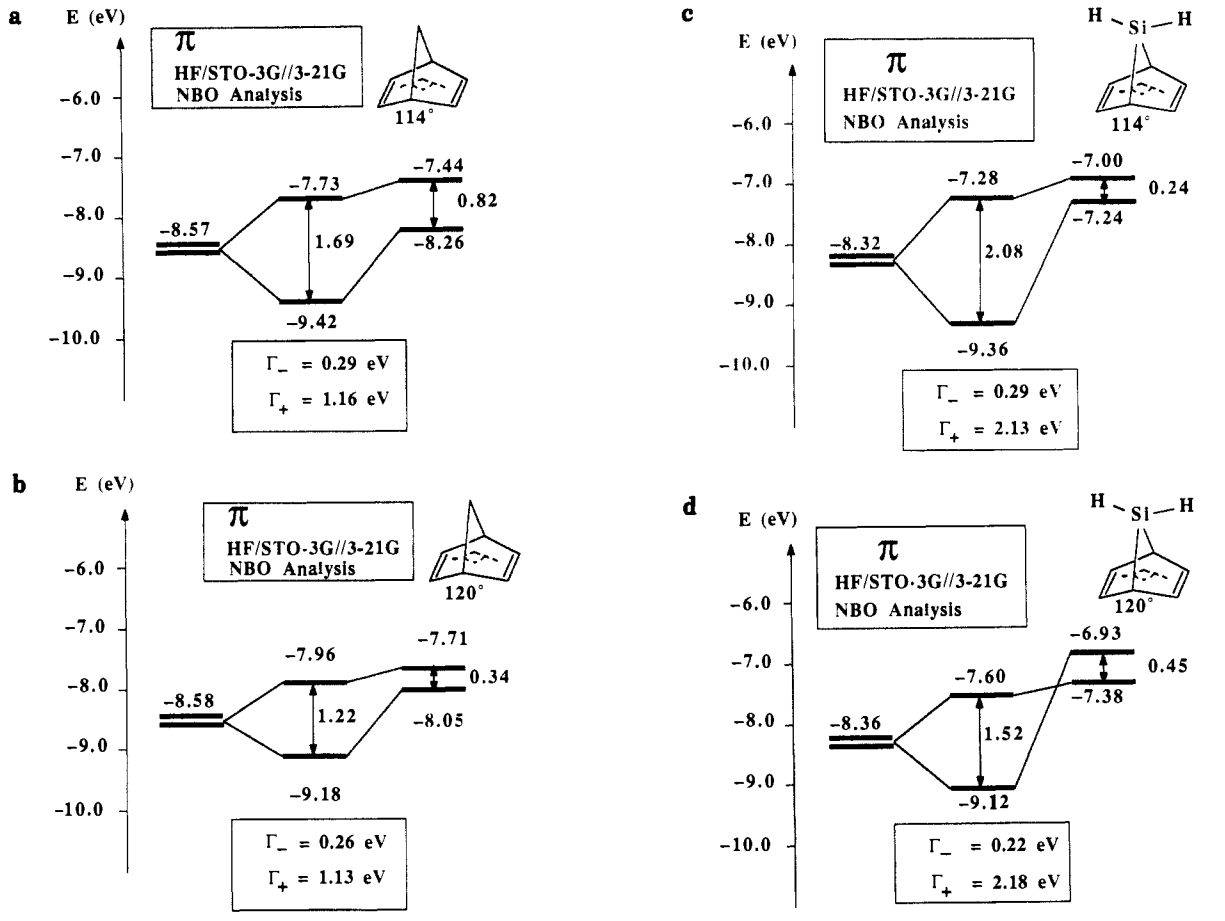

Figure 2. HF/STO-3G NBO correlation diagrams for π orbital interactions in **1** and **2**: (a) **1** (ϕ = 114°); (b) **1** (ϕ = 120°); (c) **2** (ϕ = 114°); (d) **2** (ϕ = 120°).

in terms of a localized Lewis structure. The NBOs are generated from an orthonormal set of directed natural hybrid (plus core) orbitals and are localized essentially as one or two centers (lone pairs and bonds, respectively). The NBO method is particularly well suited for analyzing TS and TB interactions in that it simultaneously generates a set comprising of both filled NBOs {core, σ, π, lone pairs} and virtual NBOs {π^*, σ^*, "Rydberg" orbitals} in such a way that the Fock matrix elements between filled and virtual LMOs are nonzero (symmetry permitting). This means that the NBO procedure enables one to analyze interactions between filled and virtual orbitals. The total set of NBOs spans the Hilbert space of the AO basis set used. The NBOs are related to the total set of CMOs (including virtuals) by a unitary transformation; thus diagonalization of the Fock matrix in the basis of the NBOs gives the complete set of CMO eigenvalues and corresponding eigenvectors (filled plus virtual). The NBO analysis has been successfully applied to dissecting both hyperconjugative[41] and TB interactions,[42] although the latter investigation was only qualitative and was based on a semiempirical wave function.

However, we should point out that problems can, and do, arise from the application of orthogonal LMOs to the analysis of orbital interactions. Such problems arise from the fact that LMOs (and NBOs) obtained from any of the above-mentioned procedures[37,40] are orthogonal. Although orbital orthogonality is a useful property, in that analysis of interactions between the LMOs is reduced to a simple Hückel-type treatment, it does have a drawback in that the LMOs cannot be truly "two-center" localized orbitals but have delocalization or "orthogonalization" tails in order to ensure their mutual orthogonality. Consequently, "pure" TS mixing of two LMOs must necessarily result in the incorporation of orbitals that are centered on atoms not conceptually involved in the TS interactions. In other words, some "TB" mixing is actually incorporated at the "TS" mixing stage, and one should treat the analysis of TS and TB interactions using LMOs schemes with some caution.[43] In this paper, we are interested mainly in trends between structurally similar molecules **1** and **2**. It is reasonable to assume, therefore, that the NBO analysis should give a consistent picture in this case. Evidence in support of this assumption is presented below.

TS and TB interactions in norbornadiene, **1**, have already been investigated by Heilbronner and Schmelzer by using Edmiston–Ruedenberg LMOs derived from semiempirical SCF wave functions (from SPINDO,[44] MINDO/2,[45] and CNDO/2[46] calculations). The NBO analysis on **1** and **2** was carried out on the 3-21G optimized structures, by using both the 3-21G and STO-3G basis sets, and the results are given in Table III. Hereafter we shall designate the π (π^*) localized NBO orbital by $^{NB}\pi$ ($^{NB}\pi^*$). For purposes of comparison, calculations were also carried out on modified geometries of **1** and **2** in which ϕ for one structure was given the optimized value of ϕ for the other structure, and vice versa. The STO-3G results were used to construct the π,π and π^*,π^* interaction diagrams shown in Figures 2 and 3, respectively (some 3-21G π,π interaction diagrams are given in the preliminary account of this work[47]). Unless stated otherwise the

(40) (a) Foster, J. P.; Weinhold, F. *J. Am. Chem. Soc.* **1980**, *102*, 7211. (b) Reed, A. E.; Weinstock, R. B.; Weinhold, F. *J. Chem. Phys.* **1985**, *83*, 735. (c) Reed, A. E.; Weinhold, F. *J. Chem. Phys.* **1985**, *83*, 1736. (d) Carpenter, J. E.; Weinhold, F. *J. Am. Chem. Soc.* **1988**, *110*, 368. (e) Reed, A. E.; Weinhold, F. *QCPE Bull.* **1985**, *5*, 141.
(41) Reed, A. E.; Schleyer, P. v. R. *J. Am. Chem. Soc.* **1987**, *109*, 7362.
(42) Weinhold, F.; Brunck, T. K. *J. Am. Chem. Soc.* **1976**, *98*, 4392.
(43) Paddon-Row, M. N.; Wong, S. S.; Jordan, K. D. *J. Chem. Soc., Perkin Trans. 2.* In press.
(44) Asbrink, L.; Fridh, C.; Lindholm, E. *J. Am. Chem. Soc.* **1972**, *94*, 5501. Fridh, C.; Asbrink, L.; Lindholm, E. *Chem. Phys. Lett.* **1972**, *15*, 282.
(45) Dewar, M. J. S.; Haselbach, E. *J. Am. Chem. Soc.* **1970**, *92*, 570.
(46) Pople, J. A.; Santry, D. P.; Segal, G. A. *J. Chem. Phys.* **1965**, *43*, 129.
(47) Paddon-Row, M. N.; Jordan, K. D. *J. Chem. Soc., Chem. Commun.* **1988**, 1508.

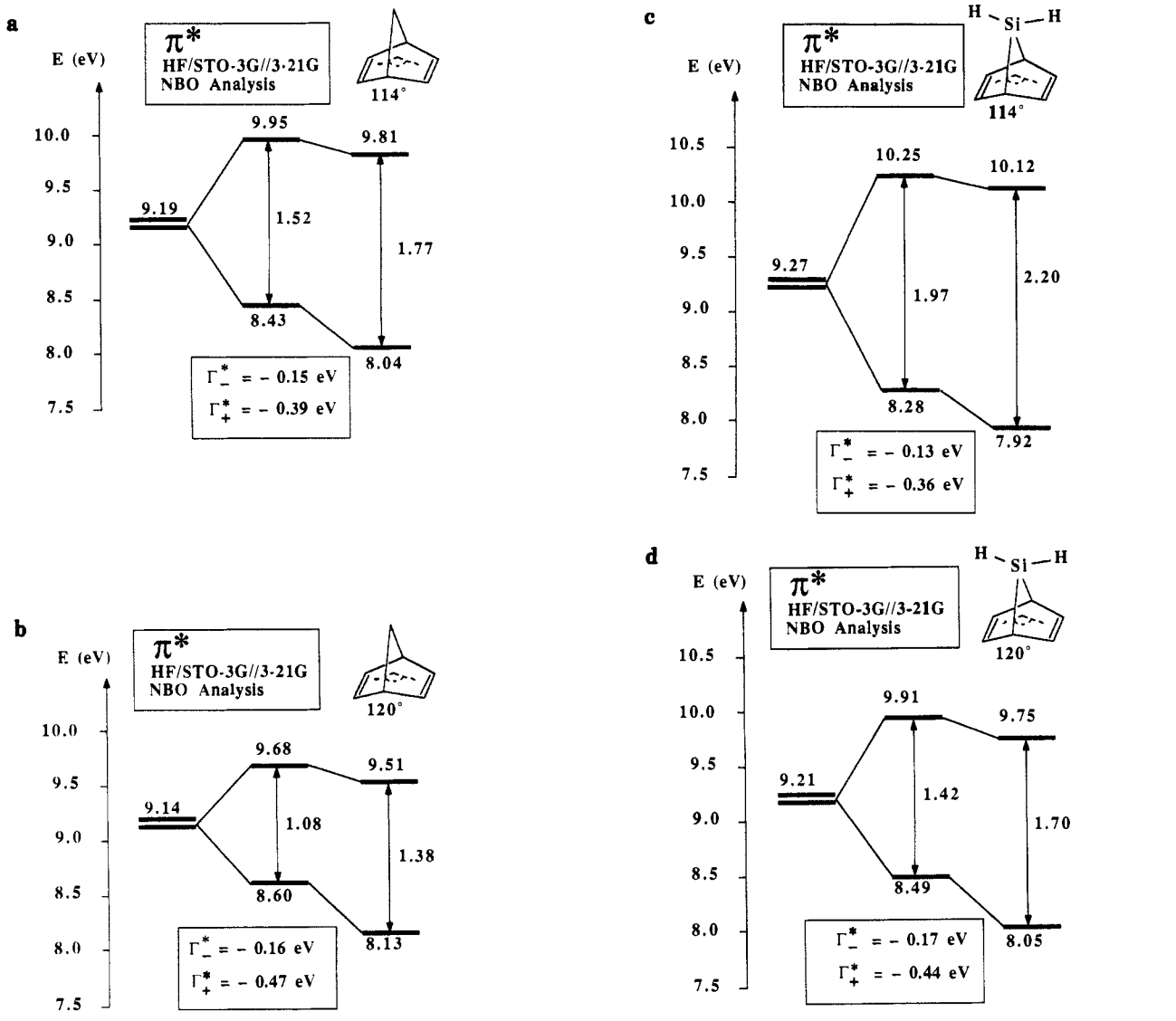

Figure 3. HF/STO-3G NBO correlation diagrams for π^* orbital interactions in **1** and **2**: (a) **1** (ϕ = 114°); (b) **1** (ϕ = 120°); (c) **2** (ϕ = 114°); (d) **2** (ϕ = 120°).

ensuing discussion refers to the STO-3G results. The 3-21G and STO-3G self-energies of the localized $^{NB}\pi_a$ and $^{NB}\pi_a^*$ NBOs, $E(^{NB}\pi_a)$ and $E(^{NB}\pi_a^*)$, respectively, are essentially independent of both the value of the dihedral angle, ϕ, and the nature of X7. Such independence is to be expected for well-localized (and transferable) orthogonal π and π^* orbitals.[48] The TS splitting energies between the $^{SL}\pi_+$ and $^{SL}\pi_-$ SLMOs (Δ_{TS}), and between the $^{SL}\pi_+^*$ and $^{SL}\pi_-^*$ SLMOs (Δ_{TS}^*), for a given value of ϕ should also be independent of X7, and the data indicate that this is approximately the case. The magnitudes of Δ_{TS} and Δ_{TS}^* for **1** and **2** fall off quite rapidly with increasing ϕ. Consequently, Δ_{TS} and Δ_{TS}^* for optimized **2** (ϕ = 120°) are ca. 0.6–0.7 eV smaller than those for **2** having a dihedral angle (ϕ = 114°) equal to that for optimized **1**. Likewise, Δ_{TS} and Δ_{TS}^* for optimized **1** (ϕ = 114°) are ca. 0.5 eV larger than those for **1** having ϕ = 120°. The dependence of Δ_{TS} and Δ_{TS}^* on ϕ in **1** and **2** provides a quantitative measure of the geometrical factor that contributes to the sequence of the π and π^* CMO levels (vide supra).

An alternative measure of Δ_{TS} and Δ_{TS}^* for **1** (ϕ = 114°) can be obtained by using the ethene dimer approach in which two ethene molecules are situated so as to mimic the disposition of the double bonds in **1**.[43] The STO-3G Δ_{TS} and Δ_{TS}^* values for this dimer are about 2.0 and 1.7 eV, respectively (see Table III of ref 43 for further details). The values are slightly larger than, but nevertheless still comparable to, those calculated by using the Weinhold NBO procedure (i.e., 1.7 and 1.5 eV for Δ_{TS} and Δ_{TS}^*, respectively). The reasonable agreement between the two methods of calculation reinforces our confidence that the above-mentioned caveat on using orthogonal LMOs is not important to the analysis discussed here.

In marked contrast to the TS interactions, TB interactions, as measured by the various Γ and Γ^* values, are practically insensitive to changes in ϕ, a result that was assumed above to be true when discussing electronic effects on TB interactions. In that discussion, it was also argued that the magnitude of Γ_- should be similar in both **1** and **2** because the energy and shape of the σ SLMO, β_3, is not influenced by the nature of X7. It is gratifying then, to see from the data of Table III that the Γ_- values for **1** and **2** differ by no more than 0.1 eV. On the other hand, for a given value of ϕ, Γ_+ is about 1 eV larger for **2** than for **1**. The value of Γ_+ for **2** is just sufficiently large enough to outweigh the combined Δ_{TS} plus Γ_- interaction energy, resulting in the observed level inversion of the π CMOs in this molecule. However, the balance is fine and reducing ϕ by only 2° in **2** causes an increase in Δ_{TS} sufficiently large enough to bring the $^{CM}\pi_+$ CMO level below the $^{CM}\pi_-$ CMO level.

Turning to interactions involving π^* orbitals, we see from Figure 3 that the net splitting energy between the π^* CMOs is actually *larger* than the Δ_{TS}^* splitting energy (the same effect is observed

(48) Bieri, G.; Dill, J. D.; Heilbronner, E.; Schmelzer, A. *Helv. Chim. Acta* **1977**, *60*, 2234. (b) Mohraz, M.; Batich, Ch.; Heilbronner, E.; Vogel, P.; Carrupt, P.-A. *Recl. Trav. Chim. Pays-Bas* **1979**, *98*, 1979. (c) Bloch, M.; Jones, T. B. *Chem. Ber.* **1979**, *112*, 3691.

Table III. HF Self-Energies for $^{NB}\pi_a(E(^{NB}\pi_a))$ and $^{NB}\pi_a^*(E(^{Nb}\pi_a^*))$, TS Interaction Matrix Elements and TS Splitting Energies between $^{NB}\pi_a$ and $^{NB}\pi_b$ ($^{NB}F_{ab}$ and Δ_{TS}) and between $^{NB}\pi_a^*$ and $^{NB}\pi_b^*$ ($^{Nb}F_{a^*b^*}$ and Δ_{TS}^*), TS Splitting Energies between Canonical MOs (Δ and Δ^*), and Total TB Contributions (Γ) for **1** and **2** as a Function of the Flap Angle ϕ[a,b]

		ϕ			
		114°		120°	
		3-21G	STO-3G[c]	3-21G	STO-3G[c]
		π Manifold			
1	$E(^{NB}\pi_a)$	−9.90	−8.57	−9.88	−8.58
	$^{NB}F_{ab}$	−0.94	−0.84	−0.71	−0.61
	Δ_{TS}	1.88	1.69	1.42	1.22
	Δ	1.04	0.82	0.60	0.34
	Γ_-	0.24	0.29	0.21	0.26
	Γ_+	1.07	1.16	1.02	1.13
	$\Gamma_- - \Gamma_+$	−0.83	−0.87	−0.81	−0.87
2	$E(^{NB}\pi_a)$	−10.09	−8.32	−10.00	−8.36
	$^{NB}F_{ab}$	−1.16	−1.04	−0.86	−0.76
	Δ_{TS}	2.32	2.08	1.73	1.52
	Δ	0.46	0.24	−0.16	−0.45
	Γ_-	0.15	0.29	0.10	0.22
	Γ_+	2.00	2.13	1.98	2.18
	$\Gamma_- - \Gamma_p$	−1.86	−1.84	−1.89	−1.96
		π^* Manifold			
1	$E(^{NB}\pi_a^*)$	6.41 [5.70][d]	9.19	6.33 [5.67][d]	9.14
	$^{NB}F_{a^*b^*}$	−0.93 [−0.90][d]	−0.76	−0.66 [−0.64][d]	−0.54
	Δ_{TS}^*	1.85 [1.80][d]	1.52	1.31 [1.28][d]	1.08
	Δ^*	1.99	1.77	1.58	1.38
	Γ_-^*	−1.06 [−0.32][d]	−0.15	−1.01 [−0.34][d]	−0.16
	Γ_+^*	−1.20 [−0.51][d]	−0.39	−1.28 [−0.63][d]	−0.47
	$\Gamma_-^* - \Gamma_+^*$	0.14 [0.19][d]	0.24	0.26 [0.29][d]	0.31
2	$E(^{NB}\pi_a^*)$	6.14 [5.53][d]	9.27	6.01 [5.41][d]	9.21
	$^{NB}F_{a^*b^*}$	−1.14 [−1.15][d]	−0.98	−0.81 [−0.79][d]	−0.71
	Δ_{TS}^*	2.29 [2.23][d]	1.97	1.63 [1.58][d]	1.42
	Δ^*	2.90	2.20	2.45	1.70
	Γ_-^*	−1.07 [−0.43][d]	−0.13	−0.99 [−0.36][d]	−0.17
	Γ_+^*	−1.69 [−1.11][d]	−0.36	−1.81 [−1.23][d]	−0.44
	$\Gamma_-^* - \Gamma_+^*$	0.62 [0.68][d]	0.23	0.82 [0.87][d]	0.27

[a] Energies in eV. [b] A positive (negative) value for Γ indicates that the appropriate symmetry adapted semilocalized π or π^* level (i.e., $^{SL}\pi_+$, $^{SL}\pi_-$, $^{SL}\pi_+^*$, or $^{SL}\pi_-^*$) is raised (lowered) by through-bond orbital interactions. [c] The STO-3G results are at the 3-21G optimized geometries. [d] Results derived from modified $^{NB}\pi^*$ NBOs (from the 3-21G basis set) obtained by mixing the original $^{NB}\pi^*$ NBOs with "Rydberg" orbitals. See text.

by using the 3-21G basis set). In other words, TS and TB effects reinforce each other in the π^* manifold. Interestingly, both Γ_-^* and Γ_+^* are negative quantities (Table III) which means that π^*/σ^* mixing (which tends to lower the π^* levels) is more important than π^*/σ mixing (which tends to raise the π^* levels). Because Γ_+^* is a larger negative quantity than Γ_-^* (by almost a factor of 3 using the STO-3G basis set), the energy gap between the $^{CM}\pi^*$ CMOs is wider than that between the $^{SL}\pi^*$ SLMOs. That Γ_+^* should be more negative than Γ_-^* is reasonable because the bridge SLMO γ_6^* (shown in Figure 1c) mixes with the $^{SL}\pi_+^*$ but not with $^{SL}\pi_-^*$. From these results, it appears then that inversion of the π^* levels in simple norbornadienes is unlikely to be found, even for large values of the flap angle ϕ.

Whereas the NBO analysis of π orbital interactions in **1** and **2** gives values of Δ_{TS}, Γ_+, and Γ_- that are relatively basis set independent, such is not the case for interactions between π^* orbitals. Thus, the 3-21G Γ_+^* and Γ_-^* values are substantially larger (by factors of ca. 7 and 4, respectively) than the STO-3G values. For **1** the $\Gamma_-^* - \Gamma_+^*$ difference is nearly the same with the two basis sets, while for **2** it is 0.6 eV larger with the 3-21G basis set. Surprisingly, the 3-21G π^* NBO basis level for **1** and **2** lies above both $^{CM}\pi_+^*$ and $^{CM}\pi_-^*$ CMOs, illustrative of which is the case of **1** (ϕ = 114°) shown in Figure 4 (solid lines). Experimentally, a different picture emerges; ET studies show that the π^* anion of ethene (1.78 eV[49]) lies almost midway between the π_+^* and π_-^* anion states of **1** (1.04 and 2.56 eV[8]). In contrast, the HF/3-21G//3-21G π^* NBO energy for ethene (5.93 eV) is still ca. 0.7 eV above the centroid of the 3-21G π_+^* and π_-^* CMO levels of **1**. However, the STO-3G interaction diagrams of Figure 3a are more consistent with experiment, since the STO-3G NBO π^* levels for **1** (ϕ = 114°) and ethene lie within 0.26 and 0.11 eV, respectively, of the centroid of the π^* CMO levels of **1**.

It is not absolutely clear why the NBO analysis with the 3-21G basis set (and presumably other split-valence shell basis sets) appears to treat π^* interactions poorly, although part of the problem seems to lie in the way in which the NBO procedure generates the π^* NBOs and the corresponding "Rydberg" outer p orbitals, associated with the C atoms of the double bonds. This is seen from the HF/3-21G//3-21G NBO data for ethene; the $^{NB}\pi^*$ NBO level (5.93 eV) lies 0.85 eV *above* the $^{CM}\pi^*$ CMO level. This is clearly unsatisfactory since the $^{NB}\pi^*$ and $^{CM}\pi^*$ levels of ethene should be the same, as indeed they are using the STO-3G minimal basis set. Inspection of the Fock matrix in the basis of the NBOs (3-21G basis set) reveals the presence of two large and equal interaction terms (3.2 eV) between the $^{NB}\pi^*$ NBO and the two "Rydberg" orbitals, one per carbon atom, which are formed mainly from the outer p orbitals of the split-valence shell basis set. Diagonalization of this 3 × 3 Fock matrix generates a new "$^{NB}\pi^*$" orbital whose energy is identical with that of the $^{CM}\pi^*$ CMO and is nearly identical with the centroid of the two HF/3-21G $^{CM}\pi^*$ CMO levels of **1** (5.28 eV; ϕ = 114°), which is in much better agreement with experiment.

Applying this promising approach to **1** and **2**[50] leads to the modified $^{NB}\pi^*$ NBOs from which TS and TB interaction energies can be derived. These results are given in Table III (in square brackets), and those for **1** (ϕ = 114°) are also shown graphically in Figure 4 (broken lines). The lowering of the $^{NB}\pi^*$ levels (by

(49) Jordan, K. D.; Burrow, P. D. *Acc. Chem. Res.* **1978**, *11*, 341.

(50) This involves the diagonalization of a pair of 9 × 9 Fock matrices for each molecule. Each matrix is associated with a particular double bond, the basis of which consists of the $^{NB}\pi^*$ NBO and eight "Rydberg" orbitals (four outer orbitals, one s and three p orbitals, per carbon atom).

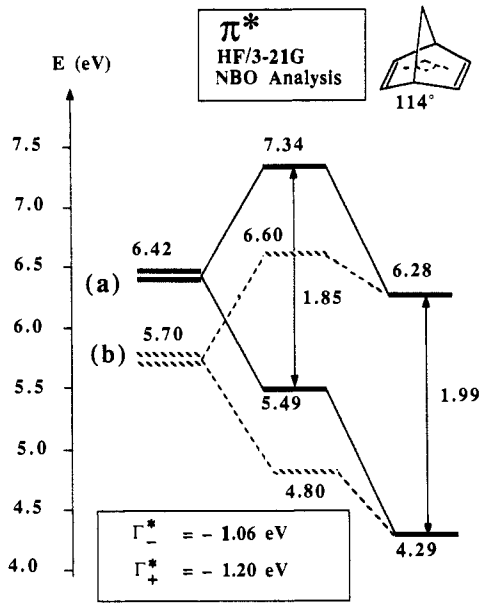

Figure 4. HF/3-21G//3-21G NBO correlation diagrams for π^* orbital interactions in **1** (ϕ = 114°) using (a) unmodified $^{NB}\pi^*$ NBOs (solid lines) and (b) modified $^{NB}\pi^*$ NBOs (broken lines) (see text).

about 0.7 eV) brought about through mixing in of the "Rydberg" orbitals also results in considerably smaller, and hence more realistic, values for Γ^*_+ and Γ^*_-. The modified absolute values of Γ^*_+ and Γ^*_- are somewhat larger than the corresponding STO-3G values (particularly in the case of Γ^*_+ for **2**). It is not known whether these differences between the magnitudes of Γ^*_+ and Γ^*_- obtained with the two basis sets is physically significant or whether it is an artifact due to the use of an extended basis set. In general, enlarging the basis set leads to unpredictable changes in the energies of virtual orbitals (which are not bound), and this is in marked contrast to the situation for filled orbitals, where energies converge to unique values as the basis set is enlarged. One consequence of this is that the separation between the (noninteracting) π^* and σ^* levels is basis set dependent and, therefore, so too will be the π^*/σ^* interaction energies. This point is supported by the observation that the 3-21G second LUMO (SLUMO) of **2** is *not* the expected $^{CM}\pi^*_-$ (a_2) CMO (this is the third LUMO) but another CMO of b_2 symmetry (see footnote f in Table I). Such a situation is not observed when using the STO-3G basis set (with which the second b_2 CMO of **2** lies 3 eV above the a_2 SLMO), nor is it observed, when using either basis set, for **1** and **3**. The 3-21G LUMO and SLUMO both contain nearly equal contributions from the π^*_+ SLMO and from SLMOs derived from the C1–Si–C4 bridge (particularly from Si); we have classified the LUMO as π^* on the grounds that the resulting 3-21G π^* splitting energy (2.45 eV) for **2** is in better agreement with the STO-3G value (1.70 eV) than the alternative assignment of the SLUMO to π^* which would then give a π^* splitting energy of only 0.04 eV. We believe that the 3-21G basis set results in a too narrow separation between the σ^* and π^* virtual orbitals, at least in **2**, leading to an anomolously large absolute value of Γ^*_+ for **2**, as noted above. It is for this reason, together with the finding that the 3-21G splitting energy Δ^*, between the π^* CMOs for **1** (1.99 eV), is substantially larger than the experimental value of 1.52 eV,[8] whereas the STO-3G value (1.77 eV) is more satisfactory, that we place more reliance on the STO-3G data for the π^* manifold.

Further insight into TB effects in **1** and **2** can be gained by using an approach similar to that suggested by the Imamura group.[36] In this approach one begins with the Fock matrix in the basis of the NBOs (or any other type of LMO for that matter) in which all of the off-diagonal, but not the diagonal elements, have been set to zero. The diagonal elements of this "blank" matrix[51] are self-energies of the NBOs in the absence of any interactions. Orbital interactions may now be explored by progressively adding appropriate off-diagonal matrix elements to the blank Fock matrix

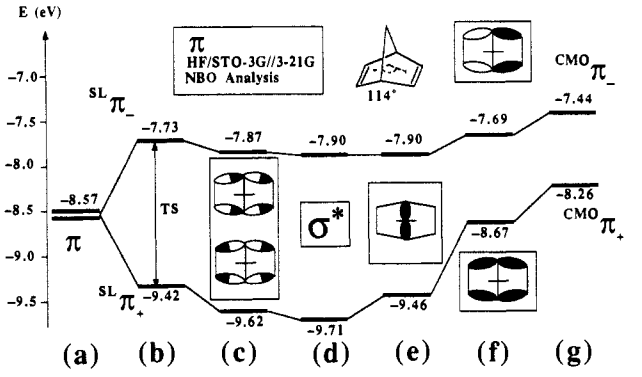

Figure 5. HF/STO-3G NBO interaction diagrams for π orbitals in **1** (ϕ = 114°). (a) The two degenerate, noninteracting $^{NB}\pi$ basis levels. (b) Inclusion of TS mixing between the two $^{NB}\pi$ levels generates the $^{SL}\pi_+$ ($\equiv \alpha_7$) and $^{SL}\pi_-$ ($\equiv \beta_5$) π SLMOs. (c) Inclusion of TB interactions involving α_8^* and β_6^* σ^* SLMOs. (d) Inclusion of *all* TB interactions involving σ^* SLMOs. (e) Inclusion of TB interactions with α_4 σ SLMOs. (f) Inclusion of TB interactions with α_2 and β_3 σ SLMOs. (g) Inclusion of *all* interactions generating the $^{CM}\pi_+$ and $^{CM}\pi_-$ CMOs. (Note: interactions with the core orbitals have been included.)

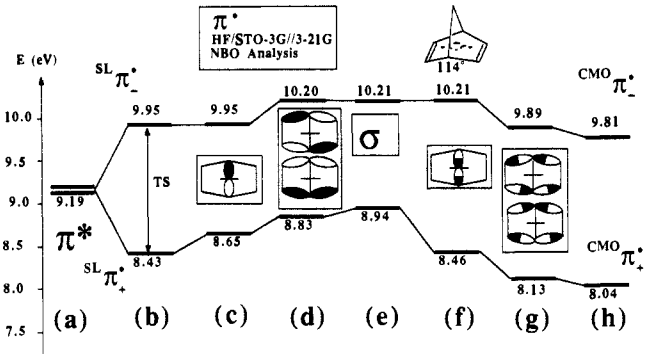

Figure 6. HF/STO-3G NBO interaction diagram for π^* orbitals in **1** (ϕ = 114°). (a) The doubly degenerate $^{NB}\pi^*$ levels (no interactions). (b) Inclusion of TS interactions between the $^{NB}\pi^*$ levels generates the $^{SL}\pi^*_+$ ($\equiv \gamma_5^*$) and $^{SL}\pi^*_-$ ($\equiv \delta_3^*$) π^* SLMOs. (c) Inclusion of TB interactions with γ_4 σ SLMO. (d) Inclusion of TB interactions with γ_1 and δ_2 SLMOs. (e) Inclusion of interaction with *all* σ SLMO. (f) Inclusion of interactions with γ_6^* σ^* SLMO. (g) Inclusion of interactions with γ_8^* and δ_4^* σ^* SLMOs. (h) Inclusion of all interactions generating the $^{CM}\pi^*_+$ and $^{CM}\pi^*_-$ CMOs. (Note: interactions with core orbitals have been included.)

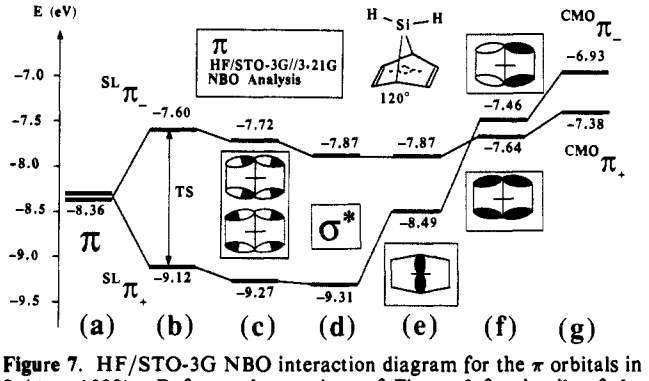

Figure 7. HF/STO-3G NBO interaction diagram for the π orbitals in **2** (ϕ = 120°). Refer to the captions of Figure 5 for details of the interaction.

and diagonalizing the resulting matrix at each step. For example, if one wishes to estimate the magnitude of interaction between orbitals ϕ_i and ϕ_j, then the matrix element $F_{ij} = \langle\phi_i|F|\phi_j\rangle$, and its conjugate, F_{ji}, are simply inserted into the blank matrix, followed by diagonalization.[36,51] The results are quantitatively

(51) Momose, T.; Tanimura, R.; Ushida, K.; Shida, T. *J. Phys. Chem.* **1987**, *91*, 5582.

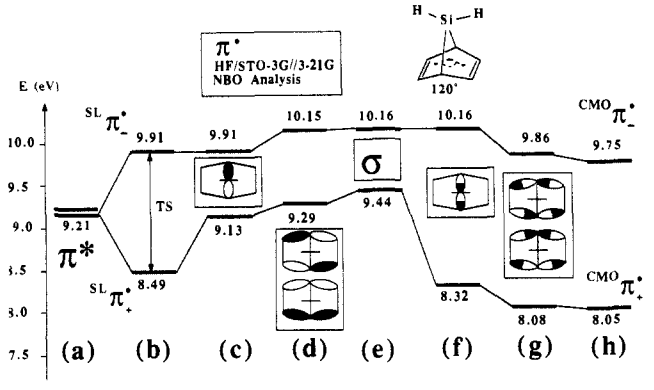

Figure 8. HF/STO-3G NBOs interaction diagram for the π^* orbitals in **2** (ϕ = 120°). Refer to the caption of Figure 6 for details of the interactions.

crude, however, but nevertheless give a useful "feel" for the relative importance of the interactions between various orbitals. Such an analysis has been carried out on **1** (ϕ = 114°) and **2** (ϕ = 120°), by using the STO-3G basis set, and the results are shown graphically in Figures 5–8. In each of these figures, step (a) → (b) represents incorporation of TS interactions.

Considering TB interactions in the π manifold (Figures 5 and 7), steps (b) → (d) represent the energy change in the $^{SL}\pi$ SLMOs due to their mixing with *all* virtual (σ^*) orbitals. Steps (d) → (g) then represent the energy change brought about by inclusion of mixing with *all* filled (σ) orbitals, (g) representing the final CMO levels. In agreement with the simple qualitative arguments given above, it is seen that mixing of $^{SL}\pi_+$ with α_2 and α_4 σ SLMOs (steps (d) → (f)) constitutes nearly all of the σ/π TB interaction energy and that this is much greater for **2** than for **1**.[52] These diagrams also illustrate very nicely the major role played by the σ SLMO, α_4, in leading to a much larger value for Γ_+ in **2**, compared to **1**. In **1** the interaction energy due to mixing with α_4 (step (d) → (e)) amounts to only 0.25 eV, compared to 0.82 eV in **2**.[53] The data for both **1** and **2** immediately reveal that σ/π mixing is energetically much more important than σ^*/π mixing and that to a good approximation the latter may be ignored. This conclusion is reassuringly in agreement with that based on other arguments.[2a,7] Of the σ^*/π mixing, that involving the α_8^* and β_6^* σ^* SLMOs[54] (step (b) → (c)) is the most important,

(52) The energy changes that accompany steps (d) → (e) and (e) → (f) in Figures 5 and 7 do not accurately reflect the respective relative contributions of SLMOs α_2 and α_4 to TB coupling with $^{SL}\pi_+$. This is because, in both **1** and **2**, step (e) → (f) includes not only the interaction matrix element between α_2 with $^{SL}\pi_+$ but also a very large interaction matrix element (ca. −5.5 eV) between α_2 and α_4. The resulting energy change accompanying step (e) → (f) is thereby increased by the presence of this term, resulting in an exaggerated contribution from α_2. This is easily seen by reversing the sequence of the steps. Thus, mixing in α_2 at step (d) → (e) results in an energy change of only 0.35 eV for **1** and 0.31 eV for **2**, compared to the respective values of 0.79 and 1.03 eV obtained through mixing of α_2 at step (e) → (f). In contrast, mixing in α_4 at step (e) → (f) results in energy changes of 0.69 eV for **1** and 1.36 eV for **2**, compared to the respective values of 0.25 and 0.82 eV obtained from the mixing of α_4 at step (d) → (e). Clearly, the C–X7–C orbitals are so strongly coupled with the orbitals of the six-membered ring in **1** and **2** that the Imamura type of energy analysis cannot give an accurate decomposition into individual contributions from the SLMOs α_2 and α_4; all one can cite with confidence is the *total* interaction energy contribution from both SLMOs. Matrix elements between other σ and σ^* SLMOs for **1** and **2** are considerably smaller than that between α_2 and α_4, and, consequently, energy changes associated with other steps in Figures 5–8 are essentially commutative.

(53) The same qualitative conclusion obtains even when the sequence of steps (d) → (e) and (e) → (f) are reversed;[52] that is, the change in the energy of π_+, through mixing with α_4, is still substantially less (0.69 eV) for **1** than for **2** (1.36 eV).

(54) Construction of the interaction diagrams of Figures 5–8 from contributions from SLMOs rather than from NBOs is easily achieved by including the right number of equivalent NBOs into each step. For example, step (b) → (c) of Figure 5 is obtained by inserting into the blank Fock matrix *all* interactions between the following six NBOs: two $^{NB}\pi$ orbitals and the four σ^* NBOs associated with the C1–C2, C3–C4, C4–C5, and C1–C6 bonds. The symmetry of the system automatically resolves the final energy changes (resulting from diagonalization of the Fock matrix) into contributions from the SLMOs (in this case, α_8^* and β_6^*).

Table IV. (STO-3G) $^{CM}\pi$ and $^{CM}\pi^*$ CMOs for **1** and **2** Expressed as Linear Combinations of the SLMOs of Figure 1[a]

$^{CM}\pi_+$:	
1	$-0.03\alpha_1 + 0.33\alpha_2 + 0.15\alpha_3 - 0.32\alpha_4 + 0.05\alpha_5 - 0.13\alpha_6 - 0.85\alpha_7$ ($\equiv^{SL}\pi_+$) $+ 0.11\alpha_8^* + 0.01\alpha_9^* - 0.03\alpha_{10}^* - 0.08\alpha_{11}^* + 0.05\alpha_{12}^*$
2	$0.02\alpha_1 + 0.29\alpha_2 + 0.22\alpha_3 - 0.48\alpha_4 - 0.09\alpha_5 - 0.02\alpha_6 - 0.78\alpha_7$ ($\equiv^{SL}\pi_+$) $+ 0.11\alpha_8^* + 0.03\alpha_9^* - 0.03\alpha_{10}^* - 0.02\alpha_{11}^* - 0.09\alpha_{12}^*$
$^{CM}\pi_-$:	
1	$0.10\beta_1 - 0.02\beta_2 - 0.20\beta_3 - 0.10\beta_4 - 0.97\beta_5$ ($\equiv^{SL}\pi_-$) $- 0.08\beta_6^* + [<0.01\beta_7^*] - 0.01\beta_8^*$
2	$0.09\beta_1 + 0.04\beta_2 - 0.21\beta_3 - 0.14\beta_4 - 0.96\beta_5$ ($\equiv^{SL}\pi_-$) $+ 0.08\beta_6^* + [<0.01\beta_7^*] - 0.07\beta_8^*$
$^{CM}\pi_+^*$:	
1	$0.09\gamma_1 + 0.02\gamma_2 - 0.03\gamma_3 + 0.12\gamma_4 - 0.94\gamma_5^*$ ($\equiv^{SL}\pi_+^*$) $+ 0.24\gamma_6^* + 0.04\gamma_7^* + 0.14\gamma_8^* - 0.06\gamma_9^* + 0.06\gamma_{10}^*$
2	$-0.07\gamma_1 + [<0.01\gamma_2] - 0.03\gamma_3 - 0.21\gamma_4 + 0.84\gamma_5^*$ ($\equiv^{SL}\pi_+^*$) $-0.47\gamma_6^* - 0.01\gamma_7^* - 0.12\gamma_8^* + 0.04\gamma_9^* - 0.06\gamma_{10}^*$
$^{CM}\pi_-^*$:	
1	$0.03\delta_1 - 0.12\delta_2 - 0.97\delta_3^*$ ($\equiv^{SL}\pi_-^*$) $- 0.18\delta_4^* + 0.06\delta_5^* - 0.07\delta_6^*$
2	$-0.03\delta_1 - 0.10\delta_2 - 0.98\delta_3^*$ ($\equiv^{SL}\pi_-^*$) $- 0.15\delta_4^* + 0.06\delta_5^* - 0.07\delta_6^*$

[a] Note that these are not the true CMOs in that contributions from the C and Si core orbitals have been ignored (see text).

representing some 70% of the total σ^*/π interaction energy.

Turning to the π^* manifold (Figures 6 and 8), it is seen that both σ^*/π^* and σ/π^* interactions are important. For example, the $^{SL}\pi_-^*$ level is raised by ca. 0.25 eV through σ/π_-^* mixing (steps (b) → (e)) and lowered by ca. 0.5 eV through σ^*/π_-^* mixing (step (e) → (h)), in both **1** and **2**. A similar pattern is also found for mixing of the σ and σ^* orbitals with the π_+^* orbitals. The data of Figures 6 and 8 therefore reinforce our arguments[10,11,15] that both σ/π^* and σ^*/π^* interactions are energetically important.

As expected from simple perturbational arguments (vide supra) the major contributors to the σ/π^* and σ^*/π^* interaction energies are γ_1, γ_4, γ_6^*, and γ_8^* (these mix with $^{SL}\pi_+^* \equiv \gamma_5^*$) and δ_2 and δ_4^* (these mix with $^{SL}\pi_-^* \equiv \delta_3^*$). Again, as in the case for the π manifold, it is the C–X7–C σ and σ^* SLMOs that are mainly responsible for the difference in magnitude of Γ_+^* between **1** and **2**: the interaction energy accompanying step (b) → (c) is about three times larger for **2** than for **1** and that accompanying step (e) – (f) is about 2.3 times as large.

An alternative way of estimating the relative contributions of the various σ and σ^* SLMOs to the TB interactions is to express the $^{CM}\pi$ and $^{CM}\pi^*$ CMOs as linear combinations of the appropriate $^{SL}\pi$ ($^{SL}\pi^*$) and σ (σ^*) SLMOs.[4] This is readily done by diagonalizing the Fock matrix in the basis of the SLMOs,[55] the resulting $^{CM}\pi$ and $^{CM}\pi^*$ eigenvectors giving the desired expressions. The percentage contribution of SLMO, ϕ_i, to the particular $^{CM}\pi$ CMO is then given by $100c_i^2$ where c_i is the coefficient associated with ϕ_i in the $^{CM}\pi$ eigenvector.[4] The data for **1** and **2** are given in Table IV. For simplicity, the Fock matrix in the basis of only the 36 SLMOs of Figure 1 was diagonalized—all C and Si core orbitals were omitted. Consequently, the $^{CM}\pi$ and $^{CM}\pi^*$ "CMOs" of Table IV are not the true CMOs, but in practice there is little difference between the two sets (the core orbital contribution to the $^{CM}\pi_+$ CMO of **1** is less than 0.01%).[56]

The data for **1** and **2** reveal that the $^{CM}\pi_-$ and $^{CM}\pi_-^*$ orbitals retain ca. 93% $^{SL}\pi_-$ and 94% $^{SL}\pi_-^*$ character, respectively. The major contribution to TB coupling in $^{CM}\pi_-$ is β_3 and β_4 in both **1** and **2**, and, as expected, contribution from the σ^* SMLOs is negligible. However, σ and σ^* SLMOs make comparable contributions to the $^{CM}\pi_-^*$, in the form of δ_2 and δ_4^*, respectively, with the δ_4^* σ^* SLMO contribution being slightly larger (ca. 3% for **1** and **2**) than δ_2 (ca. 1%), in agreement with the energetic analysis shown in Figures 6 and 7.

(55) The SLMOs are readily obtained from the NBOs by using standard techniques.[4]

(56) The energies of the "CMOs" in Table IV differ from those of the true CMOs by less than 0.03 eV.

The $^{CM}\pi_+$ CMOs of **1** and **2** contain much more TB coupling than do the $^{CM}\pi_-$ CMOs since the $^{SL}\pi_+$ character in these orbitals is only 72% in **1** and 61% in **2**. Again, these results agree with the previous analyses, the greater TB coupling observed for **2** being due largely to the α_4 σ SLMO which makes a 10% contribution to $^{CM}\pi_+$ in **1** and 23% in **2**. Through-bond coupling in $^{CM}\pi^*_+$ is somewhat less than in $^{CM}\pi_+$ since the $^{SL}\pi^*_+$ character of this CMO is 88% for **1** and 71% for **2**. These results are consistent with the data of Figures 2 and 3 which show that Γ^*_+ is less than Γ_+ in each case. The major contributions to $^{CM}\pi^*_+$ are γ_4 (1.4% in **1** and 4.4% in **2**), γ^*_6 (6% in **1** and 22% in **2**), and γ^*_8 (2% in **1** and 1.4% in **2**). Again, as for $^{CM}\pi_+$, it is the bridge SLMOs, in this case γ_4 and γ^*_6, that are largely responsible for the greater degree of TB coupling in the $^{CM}\pi^*_+$ CMO for **2**, compared to **1**. Note that, as in the case of $^{CM}\pi^*_-$, the virtual σ^* SLMOs (in this case, γ^*_6 and γ^*_8) make a greater contribution to the $^{CM}\pi^*_+$ CMO than the filled σ SLMOs, in concurrence with the data of Figures 6 and 8.

The data shown in Table IV, together with the simple perturbational MO arguments given above, nicely explain the somewhat surprising fact that both the $^{CM}\pi_-$ and $^{CM}\pi^*_-$ levels of **2** have nearly the same energies as the corresponding orbitals of **1** for all values of the dihedral angle, ϕ (see Table II). This, of course, is due largely to the fact that the C–X7–C bridge orbitals cannot contribute to the π_- and π^*_- orbitals, on grounds of symmetry. Consequently, the π_- and π^*_- orbitals are, to a first approximation, unaffected by the nature of X7. Other orbitals involving X_7 (e.g., the X_7–H orbitals in **1** and **2**) do mix with π_+ and π_- (β_4 and β_8* in the case of the former and α_3 and α_{12}* in the case of the latter). These interactions prove to be relatively unimportant in the case of the π_+ orbital. The mixing with the X_7–H bridge orbitals is somewhat more important for π_-. However, these interactions are roughly comparable in **1** and **2**; thereby shifting the π_- levels in these more or less equally.

Intriguingly, Δ_{TS} is somewhat larger than Δ^*_{TS} for **1** and **2** (Table III). This might, at first sight, seem rather surprising because the coefficients associated with the component p basis orbitals are larger in the $^{NB}\pi^*$ orbitals than in the $^{NB}\pi$ orbitals, as a result of the presence of the p orbital overlap integral, S, in the normalization factor. The ratio of the size of the coefficients in $^{NB}\pi^*$ compared to $^{NB}\pi$ is given by $(\{1 + S\}/\{1 - S\})^{1/2}$. Hence the $^{NB}\pi^*$ orbitals are better able to overlap with each other and, therefore, would be expected to produce larger TS interactions. This expectation would almost certainly be realized if the overlap between the $^{NB}\pi^*$ orbitals were restricted to overlaps between the atomic centers, C2 and C6 and between C3 and C5. Such a situation is schematized by Figure 9a. However, diagonal overlaps between C3 and C6, and between C2 and C5, are also important (cf. the C2–C6 and C2–C5 distances in **1** of 2.5 and 2.8 Å, respectively).[11,15,57] Inclusion of these overlaps into the scheme (Figure 9b) leads to a depression of the $^{SL}\pi_+$ and $^{SL}\pi^*_-$ levels (the diagonal overlaps are bonding) and to an elevation of the $^{SL}\pi_-$ and $^{SL}\pi^*_+$ levels (the diagonal overlaps are antibonding). Thus, TS interactions in norbornadienes, and in other dienes in which diagonal overlaps are important, tend to cause Δ_{TS} to be larger than Δ^*_{TS}.

Concluding Remarks

The following important points emerge from this study:

(1) The HF/3-21G and HF/STO-3G π CMOs for the optimized structures of the 7-silanorbornadienes, **2** and **3**, follow an inverted sequence, thereby implying that TB interactions are more important than TS interactions in these molecules. The 3-21G CMO splitting energies are –0.16 eV for **2** and –0.21 eV for **3**. We predict that the π-ionization bands for these molecules should show a smaller splitting than those for norbornadiene but with the vertical $^2A_1$ cation radical state lying *below* the vertical $^2B_1$ cation radical state. Indeed, UMP3/3-21G(*) and UMP3/6-31G* calculations on the $^2A_1$ and $^2B_1$ cation radical states of **2**, having the same geometry as neutral **2**, place the $^2A_1$ state about 0.27 eV in energy below the $^2B_1$ state.

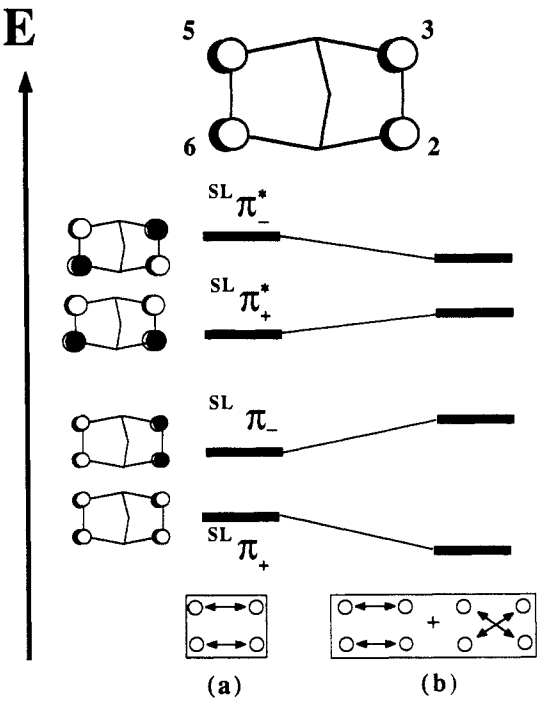

Figure 9. Schematic energy diagram for TS interactions between π orbitals and between π^* orbitals in **1** and **2**. (a) Inclusion only of overlap between p orbitals directly facing each other. (b) Inclusion of (a) type overlap plus diagonal overlaps.

(2) Dissection of π and π^* orbital interactions into TS and TB components was carried out for **1** and **2** by using the Weinhold NBO localization scheme. It was found that the inverted π CMO level sequence in **2**, compared to the natural sequence in **1**, is due to a combination of a geometric factor, which results in a weakened TS component (the 3-21G dihedral angle ϕ is 6° larger in **2** compared to **1**), and an electronic factor, which enhances TB coupling with $^{SL}\pi_+$ in **2** (silicon is more electropositive than carbon).

(3) It follows from (2) that the tendency for inversion of the π levels should become progressively stronger along the series 7-stannylnorbornadiene (X7 = SnH_2) > 7-germylnorbornadiene (X7 = GeH_2) > **2**. This predicted trend simply follows from consideration of the relative electronegativities of X7 (i.e., Si > Ge > Sn). Thus both the energy of the SLMO α_4, associated with the C1–X7–C4 bridge, and the polarization of that orbital, away from X7 and toward C1 and C4, increase along the series Si < Ge < Sn. Preliminary calculations fully support this prediction: STO-3G(*) π splitting energies for (STO-3G(*) optimized) 7-germylnorbornadiene and 7-stannylnorbornadiene are, respectively, –0.35 eV and –0.95 eV, and the levels are inverted in each case (cf. the STO-3G π splitting energy of –0.16 eV for **2**).[59]

(4) TB coupling is much more important in the $^{CM}\pi_+$ and $^{CM}\pi^*_+$ CMOs than in the $^{CM}\pi_-$ and $^{CM}\pi^*_-$ CMOs. This is due largely to the C–X7–C bridge SLMOs (α_4, α^*_{10}, γ_4, and γ^*_6). These SLMOs are also responsible for the greater degree of TB coupling observed for **2**, compared to **1**.

(5) The NBO analysis indicates that σ^*/π coupling is negligible compared to σ/π coupling and may therefore be ignored. On the contrary both σ^*/π^* and σ/π^* coupling are both important, with the former slightly predominating.

(6) Analysis of π^* orbital interactions reveal that TS and TB effects reinforce each other in both **1** and **2**. It would appear, therefore, that an inverted sequence of π^* levels is unlikely to be observed for any simple norbornadiene.

(7) The Weinhold NBO method offers a very useful approach to the analysis of TS and TB interactions in that interactions between orbitals of different occupancy can be assessed. This is more in keeping with the Hoffmann conceptual model of orbital interactions than methods based on other localization procedures[38] which generally allow only interactions between filled orbitals[37] to be analyzed.

(57) Balaji, V.; Jordan, K. D. *Chem. Phys. Lett.* **1985**, *119*, 294.

(8) The 3-21G basis set (and perhaps all split-valence shell basis sets) appears to be less satisfactory than the minimal STO-3G basis set for analyzing TB interactions involving virtual π^* orbitals. This may be due to the fact that the spacings between the π^* and σ^* manifolds are actually more realistic in the minimal basis set. Of course, if proper calculations of the anion states were carried out, for example by using the stabilization method, then the more flexible basis sets would be expected to yield more reliable results.[58]

Acknowledgment. We thank the Australian Research Grants Scheme (M.N.P.-R.) and the National Science Foundation (K.D.J.) for support of this work. We also thank the University of New South Wales for generous allocations of computing time and the Pittsburgh Supercomputing Center for a grant of time on its Cray X-MP/48 which was used for some of the calculations performed in this study.

(58) Chao, J.-S. Y.; Falcetta, M.; Jordan, K. D. Manuscript in preparation.

(59) Paddon-Row, M. N.; Wong, S. S.; Jordan, K. D. *J. Chem. Soc., Perkin Trans. 2.* In press.

A "Frustrated" Cope Rearrangement: Thermal Interconversion of 2,6-Diphenylhepta-1,6-diene and 1,5-Diphenylbicyclo[3.2.0]heptane

Wolfgang R. Roth,*,† Hans-Werner Lennartz,† W. von E. Doering,*,‡ Ludmila Birladeanu,‡ Catherine A. Guyton,‡ and Toshikazu Kitagawa‡

Contribution from the Lehrstuhl für Organische Chemie I, Ruhr-Universität, Bochum, D-4630 Bochum 1, Federal Republic of Germany, and the Department of Chemistry, Harvard University, Cambridge, Massachusetts 02138-2902. *Received May 22, 1989*

Abstract: The title reaction constitutes a reliable model of a nonconcerted, diradical mechanism closely related to a Cope rearrangement. Its activation parameters relate to a transition state approximated by 1,5-diphenylcycloheptа-1,5-diyl (**7**). Force field calculations of various conformations of the diradical model the reaction path and reproduce the "experimental" enthalpy of formation of the rate-determining transition state. The experimental enthalpy of activation of the "degenerate" Cope rearrangement of 2,5-diphenylhexa-1,5-diene-*1,6*-$^{13}C_2$ (**2**) is essentially identical with an enthalpy of activation calculated by force field for the model 1,4-diphenylcyclohexa-1,4-diyl (**6**). Strong support is thereby provided for this Cope rearrangement proceeding by a mechanism of the "continuous diradical" or "diradical-as-transition-state" type.

Diradical-Intermediated Cope Rearrangement. Skeptical of the widespread conviction that the Cope rearrangement[1] should be concerted in mechanism in all cases without exception, the suggestion was made in 1971[2] that energetics, biased more or less deliberately by employing the enthalpy of formation of the isopropyl radical being advocated at the time by Tsang,[3a] admitted the intermediacy of diradical cyclohexa-1,4-diyl (**1**) as a mechanistic alternative worthy of serious consideration. Later, when a seemingly more accurate but higher value for isopropyl radical pointed to a difference of −6.8 kcal/mol between the experimental enthalpy of formation of the transition state and the estimated enthalpy of formation of the hypothetical diradical (enthalpy of concert, $\Delta H_{ct} = \Delta_f H^* - \Delta_f H^\circ$[1]),[4b] the archetypal Cope rearrangement of hexa-1,5-diene was restored securely to the land of concert. (The energy of concert becomes −11.0 kcal/mol if a more recent value from Tsang[3c] for isopropyl radical is accepted.[5])

Wehrli, Schmid, Beluš, and Hansen[6] and Dewar and Wade[7] responded to the 1971 provocation by exploring the inference that radical-stabilizing substituents such as cyano[6] or phenyl[7a,b,c] in the 2- and 5-positions could move the mechanism into the domain of diradical-as-intermediate. The two groups found marked acceleration of rearrangement in 2,5-dicyano- and 2,5-diphenylhexa-1,5-diene (**2**), respectively, and concluded that the diradical mechanism (**6** in Scheme I) was operating. A subsequent, more thorough, thermochemical analysis of the rearrangement of **2**[4a] lent further support to the conclusion. That analysis had depended on the reliabilities of the heats of formation of styrene and α-methylstyrene[8] (used for estimation of the enthalpy of conjugation between a phenyl group and a double bond) and the heat of formation of benzyl radical as recently evaluated by Rossi and Golden.[9]

Our response to the 1971 suggestion attempts to develop a credible diradical model to compare with the Cope rearrangement. Such a model is a "frustrated" Cope rearrangement, created by

† Ruhr-Universität.
‡ Harvard University.

(1) (a) Rhoads, S. J. In *Molecular Rearrangements*; de Mayo, P., Ed.; Interscience: New York, 1963; Vol. 1, pp 655–660, 684–696. (b) Frey, H. M.; Walsh, R. *Chem. Rev.* **1969**, *69*, 103–124. (c) Gajewski, J. J. *Hydrocarbon Thermal Isomerizations*; Academic Press: New York, 1981.

(2) (a) Doering, W. von E.; Toscano, V. G.; Beasley, G. H. *Tetrahedron* **1971**, *27*, 5299–5306. (b) Doering, W. von E.; Roth, W. R.; Breuckmann, R.; Figge, L.; Lennartz, H.-W.; Fessner, W.-D.; Prinzbach, H. *Chem. Ber.* **1988**, *121*, 1–9.

(3) (a) Tsang, W. *Int. J. Chem. Kinet.* **1969**, *1*, 245–278. (b) Tsang, W. *Int. J. Chem. Kinet.* **1978**, *10*, 821–837. (c) Tsang, W. *J. Am. Chem. Soc.* **1985**, *107*, 2872–2880.

(4) (a) Doering, W. von E. *Proc. Natl. Acad. Sci. U.S.A.* **1981**, *78*, 5279–5283. (b) Doering, W. von E. In *XXIII International Congress of Pure and Applied Chemistry*; Butterworths: London, 1971; Vol. 1, 237–250.

(5) (a) Russell, J. J.; Seetula, J. A.; Gutman, D. *J. Am. Chem. Soc.* **1988**, *110*, 3092–3099. (b) Russell, J. J.; Seetula, J. A.; Timonen, R. S.; Gutman, D.; Nava, D. F. *J. Am. Chem. Soc.* **1988**, *110*, 3084–3091.

(6) (a) Wehrli, R.; Beluš, D.; Hansen, H.-J.; Schmid, H. *Nachr. Chem. Tech.* **1976**, *24*, 394–396. (b) Wehrli, R.; Beluš, D.; Hansen, H.-J.; Schmid, H. *Chimia* **1976**, *30*, 416–423. (c) Wehrli, R.; Schmid, H.; Beluš, D.; Hansen, H.-J. *Helv. Chim. Acta* **1977**, *60*, 1325–1356.

(7) (a) Dewar, M. J. S.; Wade, L. E., Jr. *J. Am. Chem. Soc.* **1973**, *95*, 290–291. (b) Wade, L. E., Jr. Ph.D. Dissertation, University of Texas at Austin; *Diss. Abstr. Intern. B* **1974**, *35*, 2106 (Order No. 74-24,946). (c) Dewar, M. J. S.; Wade, L. E., Jr. *J. Am. Chem. Soc.* **1977**, *99*, 4417–4424. (d) Dewar, M. J. S.; Ford, G. P.; McKee, M. L.; Rzepa, H. S.; Wade, L. E., Jr. *J. Am. Chem. Soc.* **1977**, *99*, 5069–5073. (e) Dewar, M. J. S.; Healy, E. F. *Chem. Phys. Lett.* **1987**, *141*, 521–524. (f) Dewar, M. J. S.; Jie, C.-X. *J. Chem. Soc., Chem. Commun.* **1987**, 1451–1453. (g) Dewar, M. J. S.; Jie, C.-X. *J. Am. Chem. Soc.* **1987**, *109*, 5893–5900. (h) In the apologia on p 5898 of ref 7g, **12** should read **10** and point 10 in Figure 4 should read 11 and vice versa.

(8) (a) Cox, J. D.; Pilcher, G. *Thermochemistry of Organic and Organometallic Compounds*; Academic Press: London, 1970. (b) Pedley, J. B.; Naylor, R. D.; Kirby, S. P. *Thermochemical Data of Organic Compounds*; Chapman and Hall: London, 1986.

(9) Rossi, M.; Golden, D. M. *J. Am. Chem. Soc.* **1979**, *101*, 1230–1235.

0002-7863/90/1512-1722$02.50/0